Pergamon

Int. J. Solids Structures Vol. 35, No. 11, pp. 1025–1055, 1998

0020–7683/98 $19.00 + .00

PII: S0020–7683(97)00107–8

STRESS FIELDS AND ENERGY RELEASE RATES IN CROSS-PLY LAMINATES

G. A. SCHOEPPNER and N. J. PAGANO
Mechanics and Surface Interactions Branch, Nonmetallic Materials Division, Materials Directorate, Air Force Research Laboratory, 2941 P Stress, Suite 1, WPAFB, OH 45433, U.S.A.
E-mail: schoepga@ml.wpafb.af.mil

(*Received* 3 *September* 1996; *in revised form* 25 *March* 1997)

Abstract—A method to model the thermoelastic response of flat laminated composites using a large radius axisymmetric hollow layered cylinder model is presented. An axisymmetric concentric cylinder model and a flat laminate model, each based on Reissner's variational principle with equilibrium stress fields, are compared. The stress components and the governing equations of the axisymmetric concentric cylinder formulation for a cylinder of infinite radius are shown analytically to be equivalent to the flat laminate formulation. Numerical results for the axisymmetric free edge stress field are shown to be nearly identical to the flat laminate free edge stress field solution. Selected results for the elastic stress fields and energy release rates in composite laminates with free edge and/or internal delaminations and transverse cracking are presented. © 1998 Elsevier Science Ltd.

INTRODUCTION

A variational theorem by Reissner (1950) is used to study the elastic stress fields in large radius axisymmetric cylinders. The variational theorem has been shown by Pagano (1978a, 1978b) to accurately describe stress fields in flat laminates. Pagano (1986, 1991, 1993) also used the theorem to describe involute bodies of revolution and concentric cylinder assemblages. Models based on this approach have been shown to accurately describe stress fields in the vicinity of stress risers and the axisymmetric model has been shown to provide accurate predictions of energy release rates. In addition, the models have the capability to provide improvements in the accuracy of the predicted stress fields by subdividing physical layers into sub-layers.

The present formulation employs the idea that the stress field in an axisymmetric cylinder approaches that in a long flat coupon as the radius to thickness ratio approaches infinity, as shown in Fig. 1, provided the flat coupon stresses are independent of the length coordinate. For cylinders with a large radius to thickness ratio, subjected to internal or external pressure and in the absence of stress concentrations, the hoop strain is nearly uniform through the wall thickness. As stated in an earlier article by Pagano (1971), if the state of stress in each layer is uniform, the response is given by classical lamination theory. The assumption of a negligible difference between the inner and outer wall hoop strain (neglecting axial end boundary effects), is a basic assumption in the well-known thin walled pressure vessel formula for homogeneous isotropic cylinders $\sigma_\theta = PR/t$ where P is either internal or external pressure. In the limit as R/t approaches infinity, the gradient of the hoop strain through the wall thickness approaches zero, generating a stress–strain field equivalent to a flat composite coupon under a uniform axial strain. Using this methodology, we can use an axisymmetric cylinder with $R \gg t$ to represent a flat laminate. The use of a hollow cylinder with $R \gg t$ to model the free edge stress field in a flat laminated composite was employed by Dandan (1988) to model off axis laminates and has been used by Sandhu *et al.* (1992) to study free edge delamination initiation in graphite epoxy laminated coupons. The capability of the existing axisymmetric formulation for modeling micromechanical damage, including interface debonding, matrix cracking and fiber breaking in brittle matrix composites as demonstrated by Pagano (1991), also makes it ideal for analyzing delamination and transverse cracks in flat laminates.

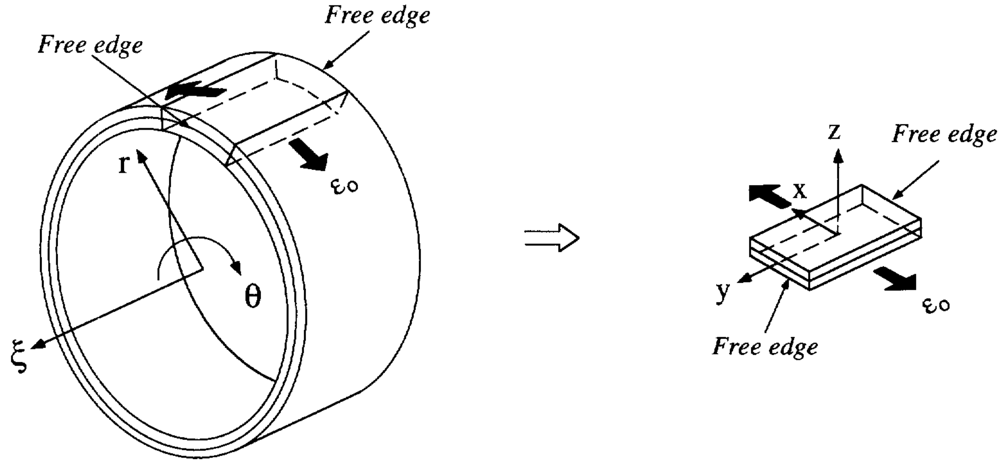

Fig. 1. Axisymmetric cylinder representation of flat laminate.

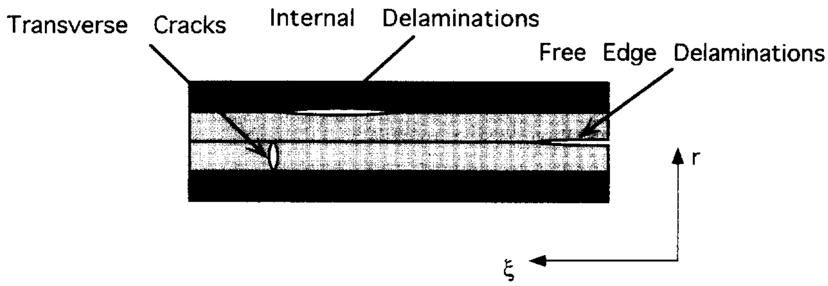

Fig. 2. Typical ply-level damage modes.

The present model, based on a modification of Pagano's (1991) formulation, employs Reissner's theorem to predict the stress fields and energy release rates for cracked flat laminates containing orthotropic layers. The model can be used to examine the initiation, propagation and interaction of damage for thermoelastic problems in flat laminates, as shown in Fig. 2. As discussed by Wang and Crossman (1980), it is widely recognized that free-edge and internal delaminations as well as transverse ply cracking in composite laminates are the most commonly observed types of damage and that delaminations typically initiate from transverse matrix cracks. This damage often results in the loss of strength and stiffness, changes in the coefficient of thermal expansion and also provides pathways for moisture or other corrosive agents. These matrix dominated failure modes can lead to fiber breakage in highly loaded plies and eventually to failure of the laminate. To understand the damage tolerance, damage resistance and reliability of composite laminates, we must first understand the formation, propagation and interaction of the various ply level damage modes.

The formulation for hollow concentric cylinders with large, but finite, radius to thickness ratios, will be presented. This formulation called the large radius cylinder model is required for computer code modeling. To show the analytical basis for modeling flat laminates using an axisymmetric formulation, a theory for cylinders with $R/t \to \infty$, based on the large radius model, is also presented. This model, called the infinite radius cylinder model, is compared to a flat laminate formulation based on the same variational principle. The infinite radius model and the flat laminate model are shown to be analytically equivalent. A numerical comparison of the large radius cylinder and the flat laminate models show that for $R/t \cong 10{,}000$, the predicted stresses are nearly identical. Predictions for crack tip stresses and energy release rates for cracked laminates are presented and compared with published results.

LARGE RADIUS CYLINDER FORMULATION

An axisymmetric variational formulation for modeling the stress field in a solid cylindrical body surrounded by concentric cylinders was developed by Pagano (1991). Theoretically, the formulation is valid for all cylinder wall thicknesses and radii. However, numerical overflow problems arise for cylinders with large radius to thickness ratios due to terms with large powers of the radial coordinate in the governing equations.

The radial geometry of a single layer hollow cylinder is described by two parameters R and t which are functions of the inner radius r_1 and outer radius r_2 as shown in Fig. 3. The parameter R is defined as the average radius of the cylinder and t is defined as the cylinder wall thickness. Then, the inner and outer radii can be expressed as

$$r_1 = R - \frac{t}{2} \quad r_2 = R + \frac{t}{2}. \tag{1}$$

A radial variable ρ is now defined in terms of the radial coordinate r and the average radius R as

$$\rho \equiv r - R \tag{2}$$

where ρ takes on values from $-t/2$ to $t/2$. Therefore, for integration in the radial direction we have

$$\int_{r_1}^{r_2} [h(r)]r^n \, \mathrm{d}r = \int_{-t/2}^{t/2} [h(R+\rho)](R+\rho)^n \, \mathrm{d}\rho \quad \text{for } n = 0, 1, 2, \ldots. \tag{3}$$

In addition, the body is bounded by axial end planes $\xi = \xi_1, \xi_2$. The surfaces $\rho = \pm t/2$ and the end planes $\xi = \xi_1, \xi_2$ may be subjected to traction and/or displacement boundary conditions that are independent of θ. Free expansion strains e_i due to a temperature change or moisture absorption are included in the formulation.

Equilibrium stress field

Stress components are represented in contracted notation for the right-handed cylindrical coordinate system (ξ, θ, r) as

$$\sigma_1 = \sigma_\xi, \quad \sigma_2 = \sigma_\theta, \quad \sigma_3 = \sigma_r, \quad \sigma_4 = \sigma_{r\theta}, \quad \sigma_5 = \sigma_{\xi r}, \quad \sigma_6 = \sigma_{\xi\theta}$$

with analogous relations for the engineering strain components. The displacement components u, v and w are in the r, θ and ξ directions, respectively. The stress components are assumed to have the form

$$\sigma_i = p_{iJ} f_{Jo}^{(i)} \quad \text{for } (i = 1\text{–}6\,; J = 1, 2, \ldots, 5) \tag{4}$$

where the functions p_{iJ} are functions of ξ only such that

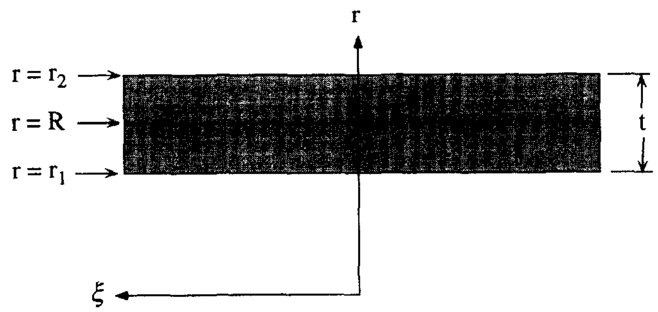

Fig. 3. Radial geometric parameters and radial variables.

$$\left.\begin{aligned} p_{i2}(\xi) &= \sigma_i\left(R+\frac{t}{2},\xi\right) \\ p_{i1}(\xi) &= \sigma_i\left(R-\frac{t}{2},\xi\right) \end{aligned}\right\} \quad \text{for } i = 1\text{–}6. \tag{5}$$

It is assumed that σ_1, σ_2 and σ_6 are linear in ρ. Substitution of these three stress components into the equilibrium equations for axisymmetry,

$$\begin{aligned} (r\sigma_3)_{,3}+r\sigma_{5,1}-\sigma_2 &= 0 \\ (r\sigma_5)_{,3}+r\sigma_{1,1} &= 0 \\ (r^2\sigma_4)_{,3}+r^2\sigma_{6,1} &= 0 \end{aligned} \tag{6}$$

defines the $f_{jo}^{(i)}$ stress shape functions for σ_3, σ_4 and σ_5 where differentiation is denoted by commas. For the present case we assume torsionless axisymmetry, so that $\sigma_4 = \sigma_6 = 0$. Since we are interested in only hollow concentric cylinders, the relationships for the core (i.e. $r_1 = 0$) (Pagano 1991) will be neglected. The stress shape functions, as derived by Pagano (1991) are written as functions of the inner radius r_1, the outer radius r_2 and the radial coordinate r. Since $r = R+\rho$, we can represent $1/r$ as a series given by

$$\frac{1}{r} = \frac{1}{R}\sum_{n=0}^{\infty}(-1)^n\frac{\rho^n}{R^n} = \frac{1}{R}\left(1-\frac{\rho}{R}+\frac{\rho^2}{R^2}-\frac{\rho^3}{R^3}+\cdots\right) \tag{7}$$

allowing the shape functions to be written in terms of R, t and ρ. Letting $f_{jo}^{(i)}$ represent the shape functions of Pagano's original formulation, and substituting (2) with (7) into the definitions of the shape functions $f_{jo}^{(i)}$, results in the following

$$\begin{aligned} f_{1o}^{(1)} &= f_{1o}^{(2)} = f_{1o}^{(3)} = \frac{r_2-r}{r_2-r_1} = \frac{t-2\rho}{2t} \\ f_{2o}^{(1)} &= f_{2o}^{(2)} = f_{2o}^{(3)} = \frac{r-r_1}{r_2-r_1} = \frac{2\rho+t}{2t} \\ f_{1o}^{(5)} &= \frac{r}{r_1}\frac{r_2-r}{r_2-r_1} \cong \frac{t-2\rho}{2t}\left(1+\frac{\rho}{R}\right) \\ f_{2o}^{(5)} &= \frac{r}{r_2}\frac{r-r_1}{r_2-r_1} \cong \frac{2\rho+t}{2t}\left(1+\frac{\rho}{R}\right) \\ f_{3o}^{(3)} &= r^3-(r_1^2+r_1r_2+r_2^2)r+r_1r_2(r_1+r_2) = (3R+\rho)\left(\rho^2-\frac{t^2}{4}\right) \\ f_{4o}^{(3)} &= r^2-(r_1+r_2)r+r_1r_2 = \left(\rho^2-\frac{t^2}{4}\right) \\ f_{5o}^{(3)} &= \frac{1}{r_1r_2r}f_4^{(3)} \cong \frac{1}{R^3}\left(1-\frac{\rho}{R}+\frac{\rho^2}{R^2}-\frac{\rho^3}{R^3}+\cdots\right)\left(\rho^2-\frac{t^2}{4}\right) \\ f_{3o}^{(5)} &= \frac{(r_1+r_2)r^2-(r_1^2+r_1r_2+r_2^2)r}{r_1^2r_2^2}+\frac{1}{r} \\ &\cong \frac{1}{R^3}\left(1-\frac{\rho}{R}+\frac{\rho^2}{R^2}-\frac{\rho^3}{R^3}+\cdots\right)\left(\frac{2}{R}\rho^3+3\rho^2-\frac{t^2}{2R}\rho-\frac{3t^2}{4}\right). \end{aligned} \tag{8}$$

Where the approximations imply $R \cong R+t$ has been invoked. We now introduce modified shape functions denoted by $f_J^{(i)}$ which are variants of $f_{Jo}^{(i)}$ and we restrict their use to the set of problems where $R \gg t$. We define

$$f_4^{(3)} = Rf_{4o}^{(3)} \quad f_5^{(3)} = R^4 f_{5o}^{(3)}$$
$$f_3^{(5)} = R^3 f_{3o}^{(5)} \quad f_3^{(3)} = f_{3o}^{(3)} \tag{9}$$

and

$$f_J^{(i)} = f_{Jo}^{(i)} \quad \text{for } (i = 1, 2, 3, 5\,; J = 1, 2). \tag{10}$$

Therefore, the present stress shape functions for torsionless axisymmetric hollow cylinders with $R \gg t$ are

$$f_1^{(1)} = f_1^{(2)} = f_1^{(3)} = \frac{t-2\rho}{2t} \quad f_2^{(1)} = f_2^{(2)} = f_2^{(3)} = \frac{2\rho+t}{2t}$$
$$f_3^{(3)} = (3R+\rho)\left(\rho^2 - \frac{t^2}{4}\right) \quad f_4^{(3)} = R\left(\rho^2 - \frac{t^2}{4}\right)$$
$$f_5^{(3)} = (R-\rho)\left(\rho^2 - \frac{t^2}{4}\right)$$
$$f_1^{(5)} = \frac{t-2\rho}{2t}\left(1+\frac{\rho}{R}\right) \quad f_2^{(5)} = \frac{2\rho+t}{2t}\left(1+\frac{\rho}{R}\right)$$
$$f_3^{(5)} = \left(1-\frac{\rho}{R}\right)\left(\frac{2}{R}\rho^3 + 3\rho^2 - \frac{t^2}{2R}\rho - \frac{3t^2}{4}\right). \tag{11}$$

Multiplying $f_{Jo}^{(i)}$ by factors of R^n to obtain $f_J^{(i)}$ in (9) reduces the magnitude of the powers of R in the governing equations, thereby reducing the likelihood of numerical overflow during implementation.

Governing equations

Using Reissner's variation formulation, Pagano (1991) derive the governing field equations in which both stresses and displacements are subject to variation. The substitution of assumed σ_{ij} into the Reissner functional gives rise to weighted displacements. The relationship between the weighted displacements from the original formulation and those from the current formulation are obtained by the use of (2) and (3). Let the weighted displacements of the current formulation be defined as

$$(\bar{q}, q^*, \hat{q}, \bar{\bar{q}}) = \int_{-t/2}^{t/2} q(1, \rho, \rho^2, \rho^3)\, \mathrm{d}\rho \tag{12}$$

where q represents displacement components u or w. If q_o represents the displacement components in the original formulation, then the relationships between the current and original weighted displacements are given by

$$\bar{q} = \bar{q}_o$$
$$q^* = q_o^* - R\bar{q}_o$$
$$\hat{q} = \hat{q}_o - 2Rq_o^* + R^2\bar{q}_o$$
$$\bar{\bar{q}} = \bar{\bar{q}}_o - 3R\hat{q}_o + 3R^2 q_o^* - R^3\bar{q}_o. \tag{13}$$

Substituting (13) into the definitions given by Pagano (1991), using (9) and neglecting terms that are negligible for $R \gg t$, leads to the strain measures,

$$\eta_{11} = \frac{R\bar{w}'}{2} + \left(\frac{1}{2} - \frac{R}{t}\right)w^{*\prime} \quad \eta_{12} = \frac{R\bar{w}'}{2} + \left(\frac{1}{2} + \frac{R}{t}\right)w^{*\prime}$$

$$\eta_{21} = \frac{\bar{u}t - 2u^*}{2t} \quad \eta_{22} = \frac{\bar{u}t + 2u^*}{2t}$$

$$\eta_{31} = \bar{u}\left(\frac{R}{t} - \frac{1}{2}\right) + \frac{2}{t}u^* \quad \eta_{32} = -\bar{u}\left(\frac{R}{t} + \frac{1}{2}\right) - \frac{2}{t}u^*$$

$$\eta_{33} = -4\bar{\bar{u}} - 12R\hat{u} - \left(6R^2 - \frac{t^2}{2}\right)u^* + Rt^2\bar{u}$$

$$\eta_{34} = -3R\hat{u} - 2R^2u^* + \frac{Rt^2}{4}\bar{u} \quad \eta_{35} = -2R^2u^*$$

$$\eta_{51} = \frac{R\bar{u}'}{2} + \left(1 - \frac{R}{t}\right)u^{*\prime} + \left(\frac{1}{2R} - \frac{2}{t}\right)\hat{u} - \frac{1}{Rt}\bar{\bar{u}} + \left(\frac{R}{t} - 1\right)\bar{w} + \left(\frac{4}{t} - \frac{1}{R}\right)w^*$$

$$\eta_{52} = \frac{R\bar{u}'}{2} + \left(1 + \frac{R}{t}\right)u^{*\prime} + \left(\frac{1}{2R} + \frac{2}{t}\right)\hat{u} + \frac{1}{Rt}\bar{\bar{u}} - \left(\frac{R}{t} + 1\right)\bar{w} - \left(\frac{4}{t} + \frac{1}{R}\right)w^*$$

$$\eta_{53} = 3R\hat{u}' - \frac{3Rt^2}{4}\bar{u}' - 6Rw^* \tag{14}$$

with all other $\eta_{iJ} = 0$. Then we have

$$\chi_{iJ} = \eta_{iJ} - E_{iJ} - s_{ijKJ}p_{jK} \quad \text{for} \begin{cases} i,j = 1,2,3,5 & \text{and} \quad J,K = 1,2 \\ i,j = 3 & \text{and} \quad J,K = 3,4,5 \\ i,j = 5 & \text{and} \quad J,K = 3 \end{cases} \tag{15}$$

where

$$E_{iJ} = \int_{-t/2}^{t/2} e_i f_J^{(i)}(R+\rho)\,\mathrm{d}\rho \tag{16}$$

and

$$s_{ijKJ} = \int_{-t/2}^{t/2} S_{ij} f_K^{(j)} f_J^{(i)}(R+\rho)\,\mathrm{d}\rho \tag{17}$$

where e_i represents the hygrothermal free expansion strains and S_{ij} are the components of the elastic compliance matrix. The constitutive equations are then given by

$$\chi_{11} = \chi_{12} = \chi_{21} = \chi_{22} = \chi_{33} = \chi_{34} = \chi_{35} = \chi_{53} = 0. \tag{18}$$

Also,

$$\mu_{31} = -\left(R - \frac{t}{2}\right)u_1 \quad \mu_{32} = \left(R + \frac{t}{2}\right)u_2$$

$$\mu_{51} = -\left(R - \frac{t}{2}\right)w_1 \quad \mu_{52} = \left(R + \frac{t}{2}\right)w_2 \tag{19}$$

with

$$\mu_{iJ} = 0 \quad \text{for} \begin{cases} i = 1,2 \quad \text{and} \quad J = 1,2 \\ i = 3 \quad \text{and} \quad J = 3,4,5 \\ i = 5 \quad \text{and} \quad J = 3 \end{cases} \tag{20}$$

where $u_1 = u(R-t/2,\xi)$, $u_2 = u(R+t/2,\xi)$, $w_1 = w(R-t/2,\xi)$ and $w_2 = w(R+t/2,\xi)$. Letting $F_{io} = 0$ represent the equilibrium equations in the original formulation, the relationships between the current and the original equilibrium equations are given by

$$\begin{aligned} F_1 &= F_{7o} + RF_{8o} \\ F_2 &= F_{8o} \\ F_3 &= F_{1o} + RF_{2o} + R^2F_{3o} + R^3F_{4o} \\ F_4 &= F_{2o} + 2RF_{3o} + 3R^2F_{4o} \\ F_5 &= F_{3o} + 3RF_{4o} \\ F_6 &= F_{4o}. \end{aligned} \tag{21}$$

Dropping terms that are negligible for $R \gg t$, the equilibrium equations

$$F_i = 0 \quad \text{for } (i = 1,2,\ldots,6) \tag{22}$$

are obtained, where

$$\begin{aligned} F_1 &= \left(\frac{1}{R}-\frac{1}{t}\right)p_{51} + \left(\frac{1}{R}+\frac{1}{t}\right)p_{52} + \frac{1}{2}(p'_{12}+p'_{11}) \\ F_2 &= -\left(\frac{3}{Rt}+\frac{3}{2R^2}\right)p_{51} + \left(\frac{3}{Rt}-\frac{3}{2R^2}\right)p_{52} + 6p_{53} - \frac{1}{t}p'_{11} + \frac{1}{t}p'_{12} \\ F_3 &= \left(\frac{1}{2}-\frac{R}{t}\right)p_{31} + \left(\frac{1}{2}+\frac{R}{t}\right)p_{32} - Rt^2p_{33} - \frac{Rt^2}{4}p_{34} + \frac{R}{2}(p'_{51}+p'_{52}) \\ &\quad - \frac{Rt^2}{4}p'_{53} - \frac{1}{2}p_{21} - \frac{1}{2}p_{22} \\ F_4 &= -\frac{2}{t}p_{31} + \frac{2}{t}p_{32} + \left(6R^2 - \frac{t^2}{2}\right)p_{33} + 2R^2p_{34} + 2R^2p_{35} \\ &\quad + \left(1-\frac{R}{t}\right)p'_{51} + \left(1+\frac{R}{t}\right)p'_{52} + \frac{1}{t}p_{21} - \frac{1}{t}p_{22} \\ F_5 &= 12Rp_{33} + 3Rp_{34} - \frac{3t^2}{4R}p_{35} + \left(\frac{1}{2R}-\frac{2}{t}\right)p'_{51} + \left(\frac{1}{2R}+\frac{2}{t}\right)p'_{52} + \left(3R+\frac{t^2}{4R}\right)p'_{53} \\ F_6 &= 4p_{33} - \frac{1}{Rt}p'_{51} + \frac{1}{Rt}p'_{52} + 2p'_{53}. \end{aligned} \tag{23}$$

Similarly if H_{io} represents the end boundary functions on $\xi = \xi_1, \xi_2$, then the current end functions are given by

$$\begin{aligned} H_1 &= H_{7o}+RH_{8o} \\ H_2 &= H_{8o} \\ H_3 &= H_{1o}+R^2H_{3o}+R^3H_{4o} \\ H_4 &= 2RH_{3o}+3R^2H_{4o} \\ H_5 &= H_{3o}+3RH_{4o}. \end{aligned} \tag{24}$$

Dropping terms that are negligible for $R \gg t$, we have

$$\begin{aligned} &H_1 = \frac{1}{2}(p_{12}+p_{11}) \quad H_2 = -\frac{1}{t}p_{11}+\frac{1}{t}p_{12} \\ &H_3 = \frac{1}{2}(p_{51}+p_{52})-\frac{t^2}{4}p_{53} \quad H_4 = \left(\frac{1}{2R}-\frac{1}{t}\right)p_{51}+\left(\frac{1}{2R}+\frac{1}{t}\right)p_{52} \\ &H_5 = \left(-\frac{1}{2R^2}-\frac{2}{Rt}\right)p_{51}+\left(-\frac{1}{2R^2}+\frac{2}{Rt}\right)p_{52}+\left(3-\frac{t^2}{4R^2}\right)p_{53}. \end{aligned} \tag{25}$$

Letting superscript k identify the layer, at a point on an interface $(R+t/2)^k=(R-t/2)^{k+1}$ $(k=1,\ldots,N-1)$, either continuity or a mixture of traction and/or displacement components may be prescribed. For continuity of tractions and displacements on an interface,

$$u_2^k = u_1^{k+1} \quad w_2^k = w_1^{k+1} \tag{26}$$

and

$$p_{32}^k = p_{31}^{k+1} \quad p_{52}^k = p_{51}^{k+1}. \tag{27}$$

Continuity of displacements (26) is satisfied for

$$\chi_{32}^k+\chi_{31}^{k+1}=0 \quad \chi_{52}^k+\chi_{51}^{k+1}=0. \tag{28}$$

Therefore, eqns (27) and (28) are the interface continuity conditions between contiguous layers. Furthermore, an interface of constant radius may be subjected to mixed boundary conditions that are consistent with the model assumptions. The following options are appropriate for prescribing tractions or displacements at a point on an interface of constant radius

$$p_{32}^k = \bar{p}_{32}^k \quad \text{or} \quad \chi_{32}^k = -\left(R+\frac{t}{2}\right)^k \bar{u}_2^k \tag{29}$$

$$p_{52}^k = \bar{p}_{52}^k \quad \text{or} \quad \chi_{52}^k = -\left(R+\frac{t}{2}\right)^k \bar{w}_2^k \tag{30}$$

$$p_{31}^k = \bar{p}_{31}^k \quad \text{or} \quad \chi_{31}^k = \left(R-\frac{t}{2}\right)^k \bar{u}_1^k \tag{31}$$

$$p_{51}^k = \tilde{p}_{51}^k \quad \text{or} \quad \chi_{51}^k = \left(R - \frac{t}{2}\right)^k \tilde{w}_1^k \tag{32}$$

where the prescribed quantities are denoted by tildes and $()^k$ implies that all variables within the () are evaluated in the kth layer. Therefore, if any σ_3, σ_5, u or w are discontinuous at an interface, the value of the discontinuous traction and/or displacements must be prescribed according to (29)–(32). Note that interface displacements appear in the governing equations only if they are prescribed, hence they are not treated as dependent variables.

To satisfy the boundary conditions on interfaces of constant ξ, one term from each of the following products (this decomposition is not unique) can be prescribed.

$$H_1^k \bar{w}_k, \quad H_2^k w_k^*, \quad H_3^k \bar{u}_k, \quad H_4^k u_k^*, \quad H_5^k \hat{u}_k. \tag{33}$$

Section continuity is implied when each member of each product of (33) is continuous. For an N layered concentric cylinder, the boundary value problem consists of $18N$ algebraic and differential equations with constant coefficients in ξ, given by six equilibrium eqns (22) and eight constitutive eqns (18) and four continuity or boundary conditions with $10N$ boundary conditions required at each $\xi = \xi_1$ and $\xi = \xi_2$. The $18N$ unknowns for the large radius cylinder model are $\bar{u}$, u^*, $\hat{u}$, $\bar{\bar{u}}$, $\bar{w}$, w^* and p_{iJ} where ($i = 1, 2, 3, 5$; $j = 1, 2$ and $i = 3$; $J = 3, 4, 5$ and $i = 5$; $J = 3$).

Rigid body displacements

The constraint of the rigid body displacement restricts the selection of totally arbitrary traction boundary conditions in boundary values problems. Therefore, the conditions under which the rigid body displacement is constrained will be examined. Consider the traction boundary value problem in which free expansion strains and all stress functions p_{iJ} vanish identically and all interfaces are continuous (actually only required for one value of ξ). From (14), $\bar{u} = \hat{u} = u^* = \bar{\bar{u}} = 0$ as well as

$$\bar{w}_k = Q_k \quad (k = 1, \ldots, N) \tag{34}$$

where

$$\left(\frac{Q}{t}\right)^{(k)} = \left(\frac{Q}{t}\right)^{(k+1)} \quad (k = 1, \ldots, N-1) \tag{35}$$

for $R \gg t$. The Q_k may be expressed in terms of one arbitrary constant. Hence the rigid body displacement components are given by (34) and (35) and specification of $\bar{w}_k$ must accompany (and replace one of) the prescribed traction boundary conditions in traction boundary value problems.

Equation (36) shows the system of six equilibrium equations and twelve constitutive equations in self-adjoint matrix form that have been coded into the large radius computer code. Since all of the field variables are not of equal order in R, the coefficients of components in the operator matrix contain powers of R ranging from $+2$ to -3.

$$
[\mathrm{A}] = \begin{bmatrix}
-s_{3311} & 0 & \frac{1}{t}-\frac{1}{2R} & -s_{1311} & -s_{1321} & -s_{2311} & -s_{2321} & -s_{3331} & -s_{3341} & -s_{3351} & 0 & -\frac{1}{3R^2t} & \frac{1}{R} & 0 & 0 & \frac{1}{t}-\frac{1}{2R} & -s_{3321} & 0 \\
0 & -s_{5511} & \frac{\mathrm{d}}{\mathrm{d}z} & 0 & 0 & 0 & 0 & 0 & 0 & 0 & -s_{5531} & 0 & 0 & \frac{1}{t}-\frac{2}{R} & \frac{1}{t}+\frac{2}{R} & 0 & 0 & -s_{5521} \\
\frac{1}{t}-\frac{1}{2R} & -\frac{\mathrm{d}}{\mathrm{d}z} & 0 & 0 & 0 & \frac{1}{2R} & \frac{1}{2R} & 2Rt & -\frac{t^2}{2} & 0 & 0 & 0 & 0 & 0 & 0 & 0 & -\frac{1}{t}-\frac{1}{2R} & 0 \\
-s_{1311} & 0 & 0 & -s_{1111} & -s_{1121} & -s_{1211} & -s_{1221} & -s_{1331} & -s_{1341} & -s_{1351} & 0 & 0 & 0 & \frac{\mathrm{d}}{\mathrm{d}z} & 0 & 0 & -s_{1321} & 0 \\
-s_{1312} & 0 & 0 & -s_{1112} & -s_{1122} & -s_{1212} & -s_{1222} & -s_{1332} & -s_{1342} & -s_{1352} & 0 & 0 & 0 & 0 & \frac{\mathrm{d}}{\mathrm{d}z} & 0 & -s_{1322} & 0 \\
-s_{2311} & 0 & \frac{1}{2R} & -s_{1211} & -s_{1221} & -s_{2211} & -s_{2221} & -s_{2331} & -s_{2341} & -s_{2351} & 0 & -\frac{1}{6R^3} & -\frac{1}{t}-\frac{1}{R} & 0 & 0 & \frac{1}{2R} & -s_{2321} & 0 \\
-s_{2312} & 0 & \frac{1}{2R} & -s_{1212} & -s_{1222} & -s_{2212} & -s_{2222} & -s_{2322} & -s_{2342} & -s_{2352} & 0 & -\frac{1}{6R^3} & \frac{1}{t}-\frac{1}{R} & 0 & 0 & \frac{1}{2R} & -s_{2322} & 0 \\
-s_{3313} & 0 & 2Rt & -s_{1313} & -s_{1323} & -s_{2313} & -s_{2323} & -s_{3333} & -s_{3343} & -s_{3353} & 0 & -\frac{4}{3} & -2R^2+\frac{t^2}{2} & 0 & 0 & -2Rt & -s_{3323} & 0 \\
-s_{3314} & 0 & -\frac{t^2}{2} & -s_{1314} & -s_{1324} & -s_{2314} & -s_{2324} & -s_{3334} & -s_{3344} & -s_{3354} & 0 & -1 & -2R^2+t^2 & 0 & 0 & -\frac{t^2}{2} & -s_{2324} & 0 \\
-s_{3315} & 0 & 0 & -s_{1315} & -s_{1325} & -s_{2315} & -s_{2325} & -s_{3335} & -s_{3345} & -s_{3355} & 0 & 0 & -2R^2 & 0 & 0 & 0 & -s_{3325} & 0 \\
0 & -s_{5513} & 0 & 0 & 0 & 0 & 0 & 0 & 0 & 0 & -s_{5533} & \frac{\mathrm{d}}{\mathrm{d}z} & 0 & 3t & -3t & 0 & 0 & -s_{5523} \\
-\frac{1}{3R^2t} & 0 & 0 & 0 & 0 & -\frac{1}{6R^3} & -\frac{1}{6R^3} & -\frac{4}{3} & -1 & 0 & -\frac{\mathrm{d}}{\mathrm{d}z} & 0 & 0 & 0 & 0 & 0 & \frac{1}{3R^2t} & 0 \\
\frac{1}{R} & 0 & 0 & 0 & 0 & -\frac{1}{t}-\frac{1}{R} & \frac{1}{t}-\frac{1}{R} & -2R^2+\frac{t^2}{2} & -2R^2+t^2 & -2R^2 & 0 & 0 & 0 & 0 & 0 & 0 & \frac{1}{R} & 0 \\
0 & \frac{1}{t}-\frac{2}{R} & 0 & -\frac{\mathrm{d}}{\mathrm{d}z} & 0 & 0 & 0 & 0 & 0 & 0 & 3t & 0 & 0 & 0 & 0 & 0 & 0 & -\frac{1}{t}+\frac{2}{R} \\
0 & \frac{1}{t}+\frac{2}{R} & 0 & 0 & -\frac{\mathrm{d}}{\mathrm{d}z} & 0 & 0 & 0 & 0 & 0 & -3t & 0 & 0 & 0 & 0 & 0 & 0 & -\frac{1}{t}-\frac{2}{R} \\
\frac{1}{t}-\frac{1}{2R} & 0 & 0 & 0 & 0 & \frac{1}{2R} & \frac{1}{2R} & -2Rt & -\frac{t^2}{2} & 0 & 0 & 0 & 0 & 0 & 0 & 0 & -\frac{1}{t}-\frac{1}{2R} & -\frac{\mathrm{d}}{\mathrm{d}z} \\
-s_{3312} & 0 & -\frac{1}{t}-\frac{1}{2R} & -s_{1312} & -s_{1322} & -s_{1312} & -s_{2322} & -s_{3332} & -s_{3342} & -s_{3352} & 0 & \frac{1}{3R^2t} & \frac{1}{R} & 0 & 0 & -\frac{1}{t}-\frac{1}{2R} & -s_{3322} & 0 \\
0 & -s_{5512} & 0 & 0 & 0 & 0 & 0 & 0 & 0 & 0 & -s_{5532} & 0 & 0 & -\frac{1}{t}+\frac{2}{R} & -\frac{1}{t}-\frac{2}{R} & \frac{\mathrm{d}}{\mathrm{d}z} & 0 & -s_{5522}
\end{bmatrix} \qquad (36a)
$$

$$[A]\begin{bmatrix} p_{31} \\ p_{51} \\ \frac{\bar{u}}{2}+\left(\frac{1}{R}-\frac{1}{t}\right)u^{*}+\left(\frac{1}{2R^2}-\frac{2}{Rt}\right)\hat{u}-\frac{1}{R^2t}\bar{u} \\ p_{11} \\ p_{12} \\ p_{21} \\ p_{22} \\ p_{33} \\ p_{34} \\ p_{35} \\ p_{53} \\ 3\hat{u}-\frac{3t^2}{4}\bar{u} \\ \frac{u^*}{R} \\ \frac{\bar{w}}{2}-\frac{1}{t}w^* \\ \frac{\bar{w}}{2}+\frac{1}{t}w^* \\ \frac{\bar{u}}{2}+\left(\frac{1}{R}+\frac{1}{t}\right)u^{*}+\left(\frac{1}{2R^2}+\frac{2}{Rt}\right)\hat{u}+\frac{1}{R^2t}\bar{u} \\ p_{32} \\ p_{52} \end{bmatrix} = \begin{bmatrix} \left(\frac{t}{2}-\frac{t^2}{12R}\right)e_3 \\ \left(\frac{t}{2}-\frac{t^2}{6R}\right)e_5 \\ 0 \\ \left(\frac{t}{2}-\frac{t^2}{12R}\right)e_1 \\ \left(\frac{t}{2}+\frac{t^2}{12R}\right)e_1 \\ \left(\frac{t}{2}-\frac{t^2}{12R}\right)e_2 \\ \left(\frac{t}{2}+\frac{t^2}{12R}\right)e_2 \\ -\left(\frac{Rt^3}{2}+\frac{t^5}{120R}\right)e_3 \\ -\frac{Rt^3}{6}e_3 \\ -\left(\frac{Rt^3}{6}-\frac{t^5}{120R}\right)e_3 \\ -\left(\frac{t^3}{2}+\frac{t^5}{40R^2}\right)e_5 \\ 0 \\ 0 \\ 0 \\ 0 \\ 0 \\ \left(\frac{t}{2}+\frac{t^2}{12R}\right)e_3 \\ \left(\frac{t}{2}+\frac{t^2}{6R}\right)e_5 \end{bmatrix} \quad (36b).$$

COMPARISON TO FLAT LAMINATE FORMULATION

Stress components

Pagano's (1978a, 1991) flat laminate formulation and the axisymmetric formulation have analogous assumptions and development. That is, in the flat laminate formulation the σ_x, σ_y and σ_{xy} stress components are assumed linear in the transverse z-direction and the form of the remaining three stress components are determined from the equilibrium equations. To enforce the same constrains in the flat laminate model that are inherent in the torsionless axisymmetric cylinder model, we assume that all stress and strain quantities

Table 1. Cartesian/cylindrical coordinate system relationships

Laminate				Cylinder		
Direction		Disp.		Direction		Disp.
1	x	u	↔	2	θ	v
2	y	v	↔	1	ξ	w
3	z	w	↔	3	r	u

Table 2. Cartesian/cylindrical stress component relationships

Flat Laminate	*Cylinder*
σ_x^+	$\sigma_2^+ = p_{22}$
σ_x^-	$\sigma_2^- = p_{21}$
σ_y^+	$\sigma_1^+ = p_{12}$
σ_y^-	$\sigma_1^- = p_{11}$
$\sigma_z^+ = p_2$	$\sigma_3^+ = p_{32}$
$\sigma_z^- = p_1$	$\sigma_3^- = p_{31}$
$\tau_{yz}^+ = s_2$	$\sigma_5^+ = p_{52}$
$\tau_{yz}^- = s_1$	$\sigma_5^- = p_{51}$

are independent of the Cartesian x-coordinate. To clarify the cylindrical coordinate system nomenclature of the cylinder model and the Cartesian coordinate system nomenclature of the flat laminate model, Tables 1 and 2 are introduced. The '+' and '−' superscripts in Table 2 refer to the top or outer and the bottom or inner surfaces, respectively. Although the same symbols are used for displacement components, *all displacement equations used here refer to either cylindrical or Cartesian coordinates, i.e., there are no mixed relations.* Therefore, this duplicity should not lead to confusion.

Using the equilibrium eqns (22) with (23) and dropping negligible terms, we can write

$$p_{33} = \frac{1}{12t}(p''_{12} - p''_{11})$$

$$p_{34} = \frac{1}{6Rt}(p'_{51} - p'_{52}) - \frac{1}{6t}(p''_{12} - p''_{11})$$

$$p_{35} = \frac{1}{R^2 t}(p_{31} - p_{32}) + \frac{1}{2R^2 t}(p_{22} - p_{21}) + \frac{1}{3Rt}(p'_{51} - p'_{52}) - \frac{1}{12t}(p''_{12} - p''_{11})$$

$$p_{53} = \frac{1}{2Rt}(p_{51} - p_{52}) - \frac{1}{6t}(p'_{12} - p'_{11}) \tag{37}$$

where differentiation with respect to the cylindrical ξ-coordinate is denoted by primes. Substituting (8) into (4), the stress components are

$$\sigma_1 = p_{11}\frac{(t-2\rho)}{2t} + p_{12}\frac{(2\rho+t)}{2t}$$

$$\sigma_2 = p_{21}\frac{(t-2\rho)}{2t} + p_{22}\frac{(2\rho+t)}{2t}$$

$$\sigma_3 = p_{31}\frac{(t-2\rho)}{2t} + p_{32}\frac{(2\rho+t)}{2t} + \left\{\frac{1}{Rt}(p_{31} - p_{32}) + \frac{1}{2Rt}(p_{22} - p_{21}) + \frac{1}{2t}(p'_{51} - p'_{52})\right\}\left(\rho^2 - \frac{t^2}{4}\right) + \frac{\rho}{6t}(p''_{12} - p''_{11})\left(\rho^2 - \frac{t^2}{4}\right) - \frac{\rho}{12t}(p''_{12} - p''_{11})\left(\frac{\rho^2}{R} - \frac{\rho^3}{R^2} + \cdots\right)\left(\rho^2 - \frac{t^2}{4}\right)$$

$$\sigma_5 = p_{51}\frac{(t-2\rho)}{2t}\left(1 + \frac{\rho}{R}\right) + p_{52}\frac{(2\rho+t)}{2t}\left(1 + \frac{\rho}{R}\right) + \left[\frac{1}{2}(p'_{11} - p'_{12}) + \frac{3}{2R}(p_{51} - p_{52})\right]\left(1 - \frac{\rho}{R} + \frac{\rho^2}{R^2} - \cdots\right)\frac{(4\rho^2 - t^2)}{4t}. \tag{38}$$

Therefore, for $R/t \to \infty$ (38) reduces to

$$\sigma_1 = p_{11}\frac{(t-2\rho)}{2t} + p_{12}\frac{(2\rho+t)}{2t}$$

$$\sigma_2 = p_{21}\frac{(t-2\rho)}{2t} + p_{22}\frac{(2\rho+t)}{2t}$$

$$\sigma_3 = p_{31}\frac{(t-2\rho)}{2t} + p_{32}\frac{(2\rho+t)}{2t} + \frac{1}{2t}(p'_{51}-p'_{52})\left(\rho^2-\frac{t^2}{4}\right) + \frac{\rho}{6t}(p''_{12}-p''_{11})\left(\rho^2-\frac{t^2}{4}\right)$$

$$\sigma_5 = p_{51}\frac{(t-2\rho)}{2t} + p_{52}\frac{(2\rho+t)}{2t} + \frac{1}{2}(p'_{11}-p'_{12})\frac{(4\rho^2-t^2)}{4t}. \tag{39}$$

From the flat laminate formulation, letting t represent the layer thickness, we write the generalized stresses as

$$N_x = \frac{t}{2}(\sigma_x^+ + \sigma_x^-) \quad N_y = \frac{t}{2}(\sigma_y^+ + \sigma_y^-)$$

$$N_z = \frac{t}{2}(\sigma_z^+ + \sigma_z^-) + \frac{t^2}{12}(\tau_{yz,y}^+ - \tau_{yz,y}^-)$$

$$V_y = \frac{t^2}{12}(\sigma_{y,y}^+ - \sigma_{y,y}^-) + \frac{t}{2}(\tau_{yz}^+ + \tau_{yz}^-)$$

$$M_x = \frac{t^2}{12}(\sigma_x^+ - \sigma_x^-) \quad M_y = \frac{t^2}{12}(\sigma_y^+ - \sigma_y^-)$$

$$M_z = \frac{t^2}{10}(\sigma_z^+ - \sigma_z^-) + \frac{t^3}{120}(\tau_{yz,y}^+ + \tau_{yz,y}^-). \tag{40}$$

Substituting (40), into the flat laminate stress relationships (eqns (8–9), Pagano 1978a) with the equilibrium equations (eqns (26), Pagano 1978a), results in the following expressions for the stresses in the flat laminate formulation

$$\sigma_y = \sigma_y^-\frac{(t-2z)}{2t} + \sigma_y^+\frac{(2z+t)}{2t}$$

$$\sigma_x = \sigma_x^-\frac{(t-2z)}{2t} + \sigma_x^+\frac{(2z+t)}{2t}$$

$$\sigma_z = \sigma_z^-\frac{(t-2z)}{2t} + \sigma_z^+\frac{(2z+t)}{2t} + \frac{1}{2}(\tau_{yz,y}^- - \tau_{yz,y}^+)\left(z^2-\frac{t^2}{4}\right) + \frac{z}{6t}(\sigma_{y,yy}^+ - \sigma_{y,yy}^-)\left(z^2-\frac{t^2}{4}\right)$$

$$\tau_{yz} = \tau_{yz}^-\frac{(t-2z)}{2t} + \tau_{yz}^+\frac{(2z+t)}{2t} + \frac{1}{2}(\sigma_{y,y}^- - \sigma_{y,y}^+)\frac{(4z^2-t^2)}{4t}. \tag{41}$$

By comparing the infinite radius cylinder model stress components (39) and the flat laminate stress components (41) it can be seen that they are equivalent.

Governing equations

The cylinder relationships given by (14), (23) and (25), have been developed for the case of $R \gg t$. As $R/t \to \infty$ (14) becomes

$$\eta_{11} = \frac{R}{2}\bar{w}' - \frac{R}{t}w^{*\prime} \quad \eta_{12} = \frac{R}{2}\bar{w}' + \frac{R}{t}w^{*\prime}$$

$$\eta_{21} = \frac{\bar{u}t - 2u^*}{2t} \quad \eta_{22} = \frac{\bar{u}t + 2u^*}{2t}$$

$$\eta_{31} = \frac{R}{t}\bar{u} \quad \eta_{32} = -\frac{R}{t}\bar{u} \quad \eta_{33} = -12R\hat{u} - 6R^2u^* + Rt^2\bar{u}$$

$$\eta_{34} = -3R\hat{u} - 2R^2u^* + \frac{Rt^2}{4}\bar{u} \quad \eta_{35} = -2R^2u^*$$

$$\eta_{51} = \frac{R}{2}\bar{u}' - \frac{R}{t}u^{*\prime} + \frac{R}{t}\bar{w} \quad \eta_{52} = \frac{R}{2}\bar{u}' + \frac{R}{t}u^{*\prime} - \frac{R}{t}\bar{w}$$

$$\eta_{53} = 3R\hat{u}' - \frac{3Rt^2}{4}\bar{u}' - 6Rw^* \tag{42}$$

with all other $\eta_{ij} = 0$, while (23) become

$$F_1 = \frac{1}{t}(p_{52} - p_{51}) + \frac{1}{2}(p'_{12} + p'_{11})$$

$$F_2 = \frac{1}{t}(p'_{12} - p'_{11}) + 6p_{53}$$

$$F_3 = \frac{R}{t}(p_{32} - p_{31}) - Rt^2p_{33} - \frac{Rt^2}{4}p_{34} + \frac{R}{2}(p'_{52} + p'_{51}) - \frac{3Rt^2}{4}p'_{53}$$

$$F_4 = 6R^2p_{33} + 2R^2p_{34} + 2R^2p_{35} + \frac{R}{t}(p'_{52} - p'_{51})$$

$$F_5 = 12Rp_{33} + 3Rp_{34} + 3Rp'_{53} \tag{43}$$

and (25) become

$$H_1 = \frac{1}{2}(p_{12} + p_{11}) \quad H_2 = \frac{1}{t}(p_{12} - p_{11})$$

$$H_3 = \frac{1}{2}(p_{52} + p_{51}) - \frac{3t^2}{4}p_{53} \quad H_4 = \frac{1}{t}(p_{52} - p_{51})$$

$$H_5 = 3p_{53}. \tag{44}$$

Note that the governing equations for the infinite radius model include one less kinematic variable, namely $\bar{u}$, and one less equilibrium equation, namely $F_6 = 0$, than the large radius cylinder model. The $\bar{u}$ terms in the strain measurements η_{33}, η_{51} and η_{52} of (14) are negligible as $R/t \to \infty$. Also, since $\bar{u}$ does not appear in the governing equations for the infinite radius model, F_6 does not exist.

Equilibrium equations

The seven equilibrium equations of the flat laminate model (eqns (26) from Pagano 1978a), are reduced to the following set of five equations if stress and strain components are independent of x.

$$N_{y,y} + \tau^+_{yz} - \tau^-_{yz} = 0$$

$$V_{y,y} + \frac{20}{t^2}M_z + \sigma^-_z - \sigma^+_z - \frac{t}{6}(\tau^-_{yz,y} + \tau^+_{yz,y}) = 0$$

$$M_{y,y} - V_y + \frac{t}{2}(\tau_{yz}^- + \tau_{yz}^+) = 0$$

$$N_z - \frac{t}{2}(\sigma_z^- + \sigma_z^+) + \frac{t^2}{12}(\tau_{yz,y}^- - \tau_{yz,y}^+) = 0$$

$$V_{y,y} + \frac{60}{t^2}M_z + 5(\sigma_z^- - \sigma_z^+) - \frac{t}{2}(\tau_{yz,y}^- + \tau_{yz,y}^+) = 0. \quad (45)$$

Substituting generalized stresses (40) into the equilibrium eqns (45) and simplifying, results in two non-trivial equations. The two non-trivial relationships, from the first and second of (45), are

$$\frac{t}{2}(\sigma_{y,y}^+ + \sigma_{y,y}^-) + \tau_{yz}^+ - \tau_{yz}^- = 0$$

$$\frac{t}{2}(\tau_{yz,y}^+ + \tau_{yz,y}^-) + \frac{t^2}{12}(\sigma_{y,yy}^+ - \sigma_{y,yy}^-) + \sigma_z^+ - \sigma_z^- = 0. \quad (46)$$

For $F_i = 0$, (43) identifies the five equilibrium equations for the infinite radius cylinder model. Substituting (37) into (43) and simplifying, yields two non-trivial equations, from $F_1 = 0$ and $F_3 = 0$. These non-trivial relationships for $R/t \to \infty$ are

$$\frac{t}{2}(p'_{12} + p'_{11}) + p_{52} - p_{51} = 0$$

$$\frac{t}{2}(p'_{52} + p'_{51}) + \frac{t^2}{12}(p''_{12} - p''_{11}) + p_{32} - p_{31} = 0. \quad (47)$$

It can be seen that the flat laminate eqns (46) are equivalent to the cylinder equations (47) for $R/t \to \infty$.

Constitutive equations

The weighted displacement field variables in the flat laminate model (Pagano, 1978a) and the cylinder model (Pagano, 1991) use the same weighted displacement nomenclature, however, different normalization was used in the two models. The relationships between the cylindrical (c) weighted displacements, using definition (12), and the flat laminate (f) weighted displacements are

$$\bar{q}_f = \frac{2}{t}\bar{q}_c \quad q_f^* = \frac{4}{t^2}q_c^* \quad \hat{q}_f = \frac{8}{t^3}\hat{q}_c. \quad (48)$$

The cylinder model (Pagano, 1991) is developed for materials that are orthotropic with respect to the ξ-direction. From small deformation theory, the laminate axial strain is $\varepsilon_x = u_{,x}$. Using the weighted displacement definitions from Pagano (1978b), the strain and curvature resultants are given by $\varepsilon_1 = (t/2)\bar{u}_{,x}$ and $\kappa_1 = (t^2/4)u^*_{,x}$, respectively. Imposing orthotropy and $\tau_{xz} = \tau_{xy} = 0$, which is the condition analogous to torsionless axisymmetry, to the flat laminate model, reduces the ten flat laminate constitutive equations (eqns (25), Pagano 1978a), to seven equations. In addition, we impose on the flat laminate model the condition that the axial strain is independent of the x coordinate (see Fig. 1) and we have

$$\varepsilon_1 - S_{11}N_x - S_{12}N_y - S_{13}N_z - te_x = 0$$

$$\frac{t}{2}\bar{v}_{,y} - S_{12}N_x - S_{22}N_y - S_{23}N_z - te_y = 0$$

$$3w^* - S_{13}N_x - S_{23}N_y - \frac{6}{5}S_{33}N_z + \frac{S_{33}t}{10}(\sigma_z^+ + \sigma_z^-) - te_z = 0$$

$$\kappa_1 - S_{11}M_x - S_{12}M_y - S_{13}M_z = 0$$

$$\frac{t^2}{4}v^*_{,y} - S_{12}M_x - S_{22}M_y - S_{23}M_z = 0$$

$$\frac{5t}{4}(3\hat{w} - \bar{w}) - S_{13}M_x - S_{23}M_y - \frac{10}{7}S_{33}M_z + \frac{t^2}{28}S_{33}(\sigma_z^+ - \sigma_z^-) = 0$$

$$\frac{3}{t}v^* + \frac{3}{4}(\bar{w}_{,y} - \hat{w}_{,y}) - \frac{6}{5t}S_{44}V_y + \frac{1}{10}S_{44}(\tau_{yz}^+ + \tau_{yz}^-) = 0 \quad (49)$$

where e_i are the engineering expansional strain components. Substituting (40) into (49) and simplifying gives

$$\varepsilon_1 - \frac{t}{2}S_{11}(\sigma_x^+ + \sigma_x^-) - \frac{t}{2}S_{12}(\sigma_y^+ + \sigma_y^-) - \frac{t}{2}S_{13}(\sigma_z^+ + \sigma_z^-) - \frac{t^2}{10}S_{13}(\tau_{yz,y}^+ - \tau_{yz,y}^-) - te_x = 0 \quad (50)$$

$$\frac{t}{2}\bar{v}_{,y} - \frac{t}{2}S_{12}(\sigma_x^+ + \sigma_x^-) - \frac{t}{2}S_{22}(\sigma_y^+ + \sigma_y^-) - \frac{t}{2}S_{23}(\sigma_z^+ + \sigma_z^-) - \frac{t^2}{12}S_{23}(\tau_{yz,y}^+ - \tau_{yz,y}^-) - te_y = 0 \quad (51)$$

$$3w^* - \frac{t}{2}S_{13}(\sigma_x^+ + \sigma_x^-) - \frac{t}{2}S_{23}(\sigma_y^+ + \sigma_y^-) - \frac{t}{2}S_{33}(\sigma_z^+ + \sigma_z^-) - \frac{t^2}{10}S_{33}(\tau_{yz,y}^+ - \tau_{yz,y}^-) - te_z = 0 \quad (52)$$

$$\kappa_1 - \frac{t^2}{12}S_{11}(\sigma_x^+ - \sigma_x^-) - \frac{t^2}{12}S_{12}(\sigma_y^+ - \sigma_y^-) - \frac{t^2}{10}S_{13}(\sigma_z^+ - \sigma_z^-) - \frac{t^3}{120}S_{13}(\tau_{yz,y}^+ + \tau_{yz,y}^-) = 0 \quad (53)$$

$$\frac{t^2}{4}v^*_{,y} - \frac{t^2}{12}S_{11}(\sigma_x^+ - \sigma_x^-) - \frac{t^2}{12}S_{12}(\sigma_y^+ - \sigma_y^-) - \frac{t^2}{10}S_{13}(\sigma_z^+ - \sigma_z^-) - \frac{t^3}{120}S_{13}(\tau_{yz,y}^+ + \tau_{yz,y}^-) = 0 \quad (54)$$

$$\frac{5t}{4}(3\hat{w} - \bar{w}) - \frac{t^2}{12}S_{13}(\sigma_x^+ - \sigma_x^-) - \frac{t^2}{12}S_{23}(\sigma_y^+ - \sigma_y^-) - \frac{3t^2}{28}S_{33}(\sigma_z^+ - \sigma_z^-) - \frac{t^3}{84}S_{13}(\tau_{yz,y}^+ + \tau_{yz,y}^-) = 0 \quad (55)$$

$$\frac{3}{t}v^* + \frac{3}{4}(\bar{w}_{,y} - \hat{w}_{,y}) - \frac{t}{10}S_{55}(\sigma_{y,y}^+ - \sigma_{y,y}^-) - \frac{1}{2}S_{44}(\tau_{yz}^+ + \tau_{yz}^-) = 0. \quad (56)$$

We obtain the analogous cylinder relations by substituting (38) and (42) into the cylinder constitutive relationships, given by

$$\chi_{iJ} = \eta_{iJ} - E_{iJ} - s_{ijKJ} p_{jK} = 0 \quad \text{for} \begin{cases} i = 1,2, & \text{and} \quad J = 1,2 \\ i = 3 & \text{and} \quad J = 3,4,5 \\ i = 5 & \text{and} \quad J = 3 \end{cases} \tag{57}$$

and assume, as in the laminate model, that the hygrothermal free expansion strain $e_5 = 0$. Furthermore, terms of the order $(R/t)^{-2}$ are neglected and we can write

$$\frac{1}{2}\bar{w}' - \frac{1}{t}w^{*\prime} - \frac{t}{6}S_{11}(p_{12}+2p_{11}) - \frac{t}{6}S_{12}(p_{22}+2p_{21}) - \frac{t}{6}S_{13}(p_{32}+2p_{31}) - \frac{t^2}{24}S_{13}(p'_{52}-p'_{51}) - \frac{t^3}{720}S_{13}(p''_{12}-p''_{11}) - \frac{t}{2}e_1 = 0 \tag{58}$$

$$\frac{1}{2}\bar{w}' + \frac{1}{t}w^{*\prime} - \frac{t}{6}S_{11}(2p_{12}+p_{11}) - \frac{t}{6}S_{12}(2p_{22}+p_{21}) - \frac{t}{6}S_{13}(2p_{32}+p_{31}) - \frac{t^2}{24}S_{13}(p'_{52}-p'_{51}) + \frac{t^3}{720}S_{13}(p''_{12}-p''_{11}) - \frac{t}{2}e_1 = 0 \tag{59}$$

$$\frac{\bar{u}}{2R} - \frac{u^*}{tR} - \frac{t}{6}S_{12}(p_{12}+2p_{11}) - \frac{t}{6}S_{22}(p_{22}+2p_{21}) - \frac{t}{6}S_{23}(p_{32}+2p_{31}) - \frac{t^2}{24}S_{23}(p'_{52}-p'_{51}) - \frac{t^3}{720}S_{23}(p''_{12}-p''_{11}) - \frac{t}{2}e_2 = 0 \tag{60}$$

$$\frac{\bar{u}}{2R} + \frac{u^*}{tR} - \frac{t}{6}S_{12}(2p_{12}+p_{11}) - \frac{t}{6}S_{22}(2p_{22}+p_{21}) - \frac{t}{6}S_{23}(2p_{32}+p_{31}) - \frac{t^2}{24}S_{23}(p'_{52}-p'_{51}) + \frac{t^3}{720}S_{23}(p''_{12}-p''_{11}) - \frac{t}{2}e_2 = 0 \tag{61}$$

$$3\hat{u}' - \frac{3t^2}{4}\bar{u}' - 6w^* + \frac{t^3}{4}S_{55}(p_{52}+p_{51}) + \frac{t^4}{20}S_{55}(p'_{21}-p'_{11}) = 0 \tag{62}$$

for $\chi_{11} = \chi_{12} = \chi_{21} = \chi_{22} = \chi_{53} = 0$, respectively. Dividing the constitutive equation $\chi_{35} = 0$ by R^2 and neglecting terms of order $(R/t)^{-1}$ and higher, we have

$$-2u^* + \frac{t^3}{12}S_{13}(p_{12}+p_{11}) + \frac{t^3}{12}S_{23}(p_{22}+p_{21}) + \frac{t^3}{12}S_{33}(p_{32}+p_{31}) + \frac{t^4}{60}S_{33}(p'_{52}-p'_{51}) + \frac{t^3}{6}e_3 = 0. \tag{63}$$

The constitutive equation $\chi_{34} = 0$ can be written as

$$-3\hat{u} + \frac{t^2}{4}\bar{u} + R\left[-2u^* + \frac{t^3}{12}S_{13}(p_{12}+p_{11}) + \frac{t^3}{12}S_{23}(p_{22}+p_{21}) + \frac{t^3}{12}S_{33}(p_{32}+p_{31}) + \frac{t^4}{60}S_{33}(p'_{52}-p'_{51}) + \frac{t^3}{6}e_3\right] = 0. \tag{64}$$

It is established in (63) that the quantity in the brackets of (64) is zero. Therefore from (64), we can write

$$-3\hat{u}+\frac{t^2}{4}\bar{u}=0 \quad \text{or} \quad \hat{u}=\frac{t^2}{12}\bar{u}. \tag{65}$$

The constitutive equation $\chi_{33}=0$ can be written as

$$\begin{aligned}-12\hat{u}+t^2\bar{u}+\frac{t^4}{120}S_{13}(p_{12}-p_{11})+\frac{t^4}{120}S_{23}(p_{22}-p_{21})+\frac{3t^4}{280}S_{33}(p_{32}-p_{31})\\ +\frac{t^5}{840}S_{33}(p'_{52}+p'_{51})+3R\left[-2u^*+\frac{t^3}{12}S_{13}(p_{12}+p_{11})+\frac{t^3}{12}S_{23}(p_{22}+p_{21})\right.\\ \left.+\frac{t^3}{12}S_{33}(p_{32}+p_{31})+\frac{t^4}{60}S_{33}(p'_{52}-p'_{51})+\frac{t^3}{6}e_3\right]=0.\end{aligned} \tag{66}$$

Again, it has been shown by (63) that the quantity in the brackets of (66) is zero, reducing (66) to

$$\begin{aligned}-12\hat{u}+t^2\bar{u}+\frac{t^4}{120}S_{13}(p_{12}-p_{11})+\frac{t^4}{120}S_{23}(p_{22}-p_{21})\\ +\frac{3t^4}{280}S_{33}(p_{32}-p_{31})+\frac{t^5}{840}S_{33}(p'_{52}+p'_{51})=0.\end{aligned} \tag{67}$$

Adding the cylinder model eqns (60) and (61), we obtain

$$\begin{aligned}\frac{\bar{u}}{R}-\frac{t}{2}S_{12}(p_{12}+p_{11})-\frac{t}{2}S_{22}(p_{22}+p_{21})-\frac{t}{2}S_{23}(p_{32}+p_{31})\\ -\frac{t^2}{12}S_{23}(p'_{52}-p'_{51})-te_2=0.\end{aligned} \tag{68}$$

The hoop strain from torsionless axisymmetry is $\varepsilon_\theta=u/r$. Using the weighted displacement definitions (12) with (7) and neglecting higher order terms in R, the strain and curvature resultants of the hoop strain are given by $\varepsilon_2=\bar{u}/R$ and $\kappa_2=u^*/R$, respectively. Substituting into (68), we get

$$\varepsilon_2-\frac{t}{2}S_{12}(p_{12}+p_{11})-\frac{t}{2}S_{22}(p_{22}+p_{21})-\frac{t}{2}S_{23}(p_{32}+p_{31})-\frac{t^2}{12}S_{23}(p'_{52}-p'_{51})-te_2=0. \tag{69}$$

Equation (69), for cylinders with $R/t\to\infty$, is equivalent to the flat laminate constitutive eqn (50). Adding the cylinder model eqns (58) and (59) we obtain

$$\bar{w}'-\frac{t}{2}S_{11}(p_{12}+p_{11})-\frac{t}{2}S_{12}(p_{22}+p_{21})-\frac{t}{2}S_{13}(p_{32}+p_{31})-\frac{t^2}{12}S_{13}(p'_{52}-p'_{51})-te_1=0 \tag{70}$$

which is equivalent to flat laminate constitutive eqn (51). Flat laminate constitutive eqn (52) is obtained by multiplying cylinder eqn (63) by $-6/t^2$. Using cylinder eqns (47), (60) and (61) with the definition of κ_2, we obtain an expression that is equivalent to the flat laminate constitutive eqn (53). Similarly, using (47), (58) and (59) we get (54). Flat laminate constitutive eqn (55) is obtained using (65) and (67). Finally, flat laminate constitutive eqn (56) is obtained using (62). Therefore, it has been shown that the seven flat laminate constitutive equations can be obtained from the infinite radius cylinder model constitutive equations.

Prescribed interface boundary displacements

Using (40), the four flat laminate prescribed interface displacement boundary relationships (from equations (28), Pagano 1978a), for assumed x-coordinate stress and strain independence can be written as

$$-\tilde{v}_1+\frac{1}{2}\bar{v}-\frac{3}{2}v^*-\frac{h}{8}\bar{w}_{,y}-\frac{t}{4}w^*_{,y}+\frac{3t}{8}\hat{w}_{,y}-\frac{t}{12}S_{44}(\tau^-_{yz}-\tau^+_{yz})+\frac{t^2}{120}S_{44}(\sigma^+_{y,y}-\sigma^-_{y,y})=0 \quad (71)$$

$$\tilde{v}_2-\frac{1}{2}\bar{v}-\frac{3}{2}v^*-\frac{h}{8}\bar{w}_{,y}+\frac{t}{4}w^*_{,y}+\frac{3t}{8}\hat{w}_{,y}+\frac{t}{12}S_{44}(\tau^-_{yz}-\tau^+_{yz})+\frac{t^2}{120}S_{44}(\sigma^+_{y,y}-\sigma^-_{y,y})=0 \quad (72)$$

$$-\tilde{w}_1-\frac{3}{4}\bar{w}-\frac{3}{2}w^*+\frac{15}{4}\hat{w}-\frac{t}{140}S_{33}(\sigma^+_z-\sigma^-_z)+\frac{t^2}{420}S_{33}(2\tau^+_{yz,y}-5\tau^-_{yz,y})=0 \quad (73)$$

$$\tilde{w}_2+\frac{3}{4}\bar{w}-\frac{3}{2}w^*-\frac{15}{4}\hat{w}+\frac{t}{140}S_{22}(\sigma^+_z-\sigma^-_z)+\frac{t^2}{420}S_{33}(5\tau^+_{yz,y}-2\tau^-_{yz,y})=0. \quad (74)$$

The infinite radius cylinder model prescribed interface displacement boundary conditions are given by

$$-\tilde{w}_1+\frac{\bar{u}'}{2}-\frac{u^{*\prime}}{t}+\frac{\bar{w}}{t}-\frac{t}{6}S_{55}(p_{52}+2p_{51})-\frac{t^2}{24}S_{55}(p'_{12}-p'_{11})=0 \quad (75)$$

$$\tilde{w}_2+\frac{\bar{u}'}{2}+\frac{u^{*\prime}}{t}-\frac{\bar{w}}{t}-\frac{t}{6}S_{55}(2p_{52}+p_{51})-\frac{t^2}{24}S_{55}(p'_{12}-p'_{11})=0 \quad (76)$$

$$-\tilde{u}_1+\frac{\bar{u}}{t}-\frac{t}{6}S_{13}(p_{12}+2p_{11})-\frac{t}{6}S_{23}(p_{22}+2p_{21})-\frac{t}{6}S_{33}(p_{32}+2p_{31})$$
$$-\frac{t^2}{24}S_{33}(p'_{52}-p'_{51})-\frac{t^3}{720}S_{33}(p''_{12}-p''_{11})=0 \quad (77)$$

$$\tilde{u}_2-\frac{\bar{u}}{t}-\frac{t}{6}S_{13}(2p_{12}+p_{11})-\frac{t}{6}S_{23}(2p_{22}+p_{21})-\frac{t}{6}S_{33}(2p_{32}+p_{31})$$
$$-\frac{t^2}{24}S_{33}(p'_{52}-p'_{51})+\frac{t^3}{720}S_{33}(p''_{12}-p''_{11})=0. \quad (78)$$

From (62) we can write

$$\frac{\bar{u}'}{2}=-\frac{4}{t^2}w^*+\frac{2}{t^2}\hat{u}'+\frac{t}{6}S_{55}(p_{52}+p_{51})+\frac{t^2}{30}S_{55}(p'_{12}-p'_{11}). \quad (79)$$

This can be expressed as

$$\frac{\bar{u}'}{2}=\frac{3\bar{u}'}{4}-\frac{\bar{u}'}{4}=-\frac{6}{t^2}w^*+\frac{3}{t^2}\hat{u}'-\frac{1}{4}\bar{u}'+\frac{t}{4}S_{55}(p_{52}+p_{51})+\frac{t^2}{20}S_{55}(p'_{12}-p'_{11}). \quad (80)$$

Substituting $\bar{u}'/2$ given in (80) into (75) leads to

$$-\tilde{w}_1+\frac{3}{t^2}\hat{u}'-\frac{u^{*\prime}}{t}-\frac{\bar{u}'}{4}-\frac{6}{t^2}w^*+\frac{\bar{w}}{t}+\frac{t}{12}S_{55}(p_{52}-p_{51})+\frac{t^2}{120}S_{55}(p'_{12}-p'_{11})=0 \quad (81)$$

which is equivalent to flat laminate prescribed displacement boundary eqn (71).

Similarly, substituting $\bar{u}'/2$ given in (80) into (76) leads to

$$\tilde{w}_2+\frac{3}{t^2}\hat{u}'+\frac{u^{*\prime}}{t}-\frac{\bar{u}'}{4}-\frac{6}{t^2}w^*-\frac{\bar{w}}{t}-\frac{t}{12}S_{55}(p_{52}-p_{51})+\frac{t^2}{120}S_{55}(p'_{12}-p'_{11})=0 \quad (82)$$

which is equivalent to the flat laminate prescribed displacement boundary eqn (72).

The recovery of the transverse/radial prescribed displacement boundary relationships requires a greater effort. Multiplying (63) by $3/t^2$ and adding the results to (77) gives

$$-\tilde{u}_1-\frac{6}{t^2}u^*+\frac{\bar{u}}{t}+\frac{t}{12}S_{13}(p_{12}-p_{11})+\frac{t}{12}S_{23}(p_{22}-p_{21})+\frac{t}{12}S_{33}(p_{32}-p_{31})$$
$$+\frac{t^2}{120}S_{33}(p'_{52}-p'_{51})-\frac{t^3}{720}S_{33}(p''_{12}-p''_{11})=0. \quad (83)$$

Using equilibrium eqns (47), this can be expressed as

$$-\tilde{u}_1-\frac{6}{t^2}u^*+\frac{\bar{u}}{t}+\frac{t}{12}S_{13}(p_{12}-p_{11})+\frac{t}{12}S_{23}(p_{22}-p_{21})$$
$$+\frac{t}{10}S_{33}(p_{32}-p_{31})+\frac{t^2}{60}S_{33}p'_{52}=0. \quad (84)$$

Equation (67) can be rewritten as

$$-\frac{\bar{u}}{t}=-\frac{12}{t^3}\hat{u}+\frac{t}{120}S_{13}(p_{12}-p_{11})+\frac{t}{120}S_{23}(p_{22}-p_{21})$$
$$+\frac{3t}{280}S_{33}(p_{32}-p_{31})+\frac{t^2}{840}S_{13}(p'_{52}+p'_{51})=0. \quad (85)$$

Thus we can write

$$-\frac{\bar{u}}{t}=-\frac{5\bar{u}}{2t}+\frac{3\bar{u}}{2t}=-\frac{30}{t^3}\hat{u}+\frac{3\bar{u}}{2t}+\frac{t}{48}S_{13}(p_{12}-p_{11})+\frac{t}{48}S_{23}(p_{22}-p_{21})$$
$$+\frac{3t}{112}S_{33}(p_{32}-p_{31})+\frac{t^2}{336}S_{13}(p'_{52}+p'_{51})=0. \quad (86)$$

Substituting $\bar{u}/t$ given in (86) into (84) gives

$$-\tilde{u}_1-\frac{6}{t^2}u^*+\frac{30}{t^3}\hat{u}-\frac{3\bar{u}}{2t}+\frac{t}{16}S_{13}(p_{12}-p_{11})+\frac{t}{16}S_{23}(p_{22}-p_{21})$$
$$+\frac{41t}{560}S_{33}(p_{32}-p_{31})+\frac{t^2}{1680}S_{33}(23p'_{52}-5p'_{51})=0. \quad (87)$$

From (65) and (67) we get

$$\frac{t^4}{120}S_{13}(p_{12}-p_{11})+\frac{t^4}{120}S_{23}(p_{22}-p_{21})+\frac{3t^4}{280}S_{33}(p_{32}-p_{31})+\frac{t^5}{840}S_{33}(p'_{52}+p'_{51}) = 0. \tag{88}$$

Using (87) and (88), we get

$$-\tilde{u}_1-\frac{3}{2t}\bar{u}-\frac{6}{t^2}u^*+\frac{30}{t^3}\hat{u}-\frac{t}{140}S_{33}(p_{32}-p_{31})+\frac{t^2}{420}(2p'_{52}-5p'_{51}) = 0 \tag{89}$$

which, recalling (48), is equivalent to the flat laminate boundary displacement eqn (73). Similarly

$$\tilde{u}_2+\frac{3}{2t}\bar{u}-\frac{6}{t^2}u^*-\frac{30}{t^3}\hat{u}+\frac{t}{140}S_{33}(p_{32}-p_{31})+\frac{t^2}{420}(5p'_{52}-2p'_{51}) = 0 \tag{90}$$

which, recalling (48), is equivalent to (74). The flat laminate interface displacement continuity conditions (from equations (27), Pagano 1978a) are readily obtained from the infinite radius cylinder model using the same procedure that was used to show equivalence of the prescribed interface displacement boundary conditions.

Generalized stress relationships

The relationships between the generalized stresses of the flat laminate model and the infinite radius cylinder model will now be investigated. Beside the obvious relationships shown in Table 2, the relationships between p_{33}, p_{34}, p_{35} and p_{53} and the flat laminate generalized stresses are considered.

Comparing equivalent equilibrium equations for the flat laminate and infinite radius cylinder models allows us to investigate the relationships between the field variables for the two models. It can be shown by equating the cylinder model F_2 function of (43) with the fifth of flat laminate eqns (26) from Pagano (1978a), that

$$p_{53} = \frac{1}{t^2}(p_{51}+p_{52})-\frac{2}{t^3}V_y. \tag{91}$$

Similarly, equating F_3, F_4 and F_5 with the third, sixth and seventh of flat laminate eqns (26) from Pagano (1978a), respectively, gives

$$t^2p_{33}+\frac{t^2}{4}p_{34} = -\frac{30}{t^3}M_z+\frac{5}{2t}(p_{32}-p_{31}) \tag{92}$$

$$6Rp_{33}+2Rp_{34}+2Rp_{35} = \frac{12}{t^3}N_z-\frac{6}{t^2}(p_{32}+p_{31})-\frac{2}{t}(p'_{52}-p'_{51}) \tag{93}$$

$$12p_{33}+3p_{34} = -\frac{12}{t^3}V'_y+\frac{360}{t^5}M_z-\frac{30}{t^3}(p_{32}-p_{31})-\frac{5}{t^2}(p'_{52}+p'_{51}). \tag{94}$$

It is seen that (92) and (94) are linearly dependent in p_{33} and p_{34}. Therefore, p_{33}, p_{34} and p_{35} cannot be explicitly expressed in terms of the flat laminate field variables. However, through the use of (92) through (94), the flat laminate generalized transverse stresses can be expressed in terms of the cylindrical field variables.

MODEL VALIDATION

The infinite radius cylinder model and the flat laminate model have been shown to be analytically equivalent. However, the infinite radius cylinder model would require a change in variables to reduce to the flat laminate mode. Therefore, the large radius cylinder model is used to approximate the infinite radius cylinder in solving boundary value problems.

For modeling problems analogous to a flat laminate subjected to a uniform axial strain, the cylinder is subjected to a small positive traction on its exterior while the interior is traction free, inducing a tensile hoop strain in the cylinder. This method of inducing a uniform hoop strain is only required for modeling flat laminate problems in which the constant y and constant z boundaries are subjected to homogeneous boundary conditions. However, the cylinder model is valid for mixed boundary conditions, consistent with the model assumptions, on any surface of constant radius and on any surface on which ξ is constant. Therefore, the model is not limited to analyzing problems in which the primary loading is in the circumferential direction. Flat laminate problems that have symmetry about both the y and z axes in which there is no applied traction and/or displacement loading in the x direction, can be modeled with the large radius model using quarter symmetry by constraining radial and axial displacements. As an example, this modeling technique can be used to develop representative volume elements for transverse cracking analysis and for analyzing pressurized crack problems.

A comparison of the numerical predictions from the large radius cylinder model and the flat laminate formulation for a laminated free edge coupon will be presented. The material properties are taken from Pagano (1978a), where the engineering moduli in the planes of elastic symmetry of each layer are given by

$$E_{11} = 20 \times 10^6 \text{ psi}$$

$$E_{22} = E_{33} = 2.1 \times 10^6 \text{ psi}$$

$$G_{12} = G_{13} = G_{23} = 0.85 \times 10^6 \text{ psi}$$

$$\nu_{12} = \nu_{13} = \nu_{23} = 0.21.$$

We consider a comparison of the large radius cylinder and flat laminate free edge stress field predictions for a four layer cross-ply laminate $[0/90]_s$ in which the layers are of equal thickness t. The width of the laminate is $2b = 16t$. The laminate is modeled with $N = 6$ where N is the number of layers in one-half of the laminate thickness. Therefore, $N = 6$ implies that each physical layer of thickness t is modeled as three sub-layers, each of thickness $t/3$.

The flat laminate formulation allows the use of quarter symmetry to model the laminate while the axisymmetric model, with external pressure loading to induce a hoop strain, requires the use of half symmetry to model the entire laminate thickness. Therefore, for $N = 6$, the flat laminate model uses six sub-layers while the axisymmetric model uses 12 sublayers.

We let the total laminate average radius be denoted by $\bar{R}$ and the total laminate thickness by T which for the present case equals $4t$. To investigate the validity of using the large radius cylinder model to analyze flat laminates, four models with different $\bar{R}/T$ ratios are examined. A comparison of the flat laminate results and the axisymmetric cylinder results for $\bar{R}/T$ ratios ranging from 100 to 100,000 are shown in Figs 4–6. Figure 4 shows the distribution of the transverse normal stress at the 90/90 interface as a function of the laminate width. The axisymmetric results quickly converge to the flat laminate results at $\bar{R}/T$ of 10,000 the results are nearly identical to the flat laminate results. Similarly, Figs 5 and 6 show the distribution of the transverse normal and transverse shear stresses at the 0/90 interface.

In Figs 4 and 5, it can be seen that the artificial external pressure is not negligible for $\bar{R}/T$ values of 100 and 1,000. In Fig. 4, the differences between the normalized flat laminate stress and the normalized stresses for $\bar{R}/T$ of 100 and 1,000 at $y/b = 0$ are 0.0543255 and

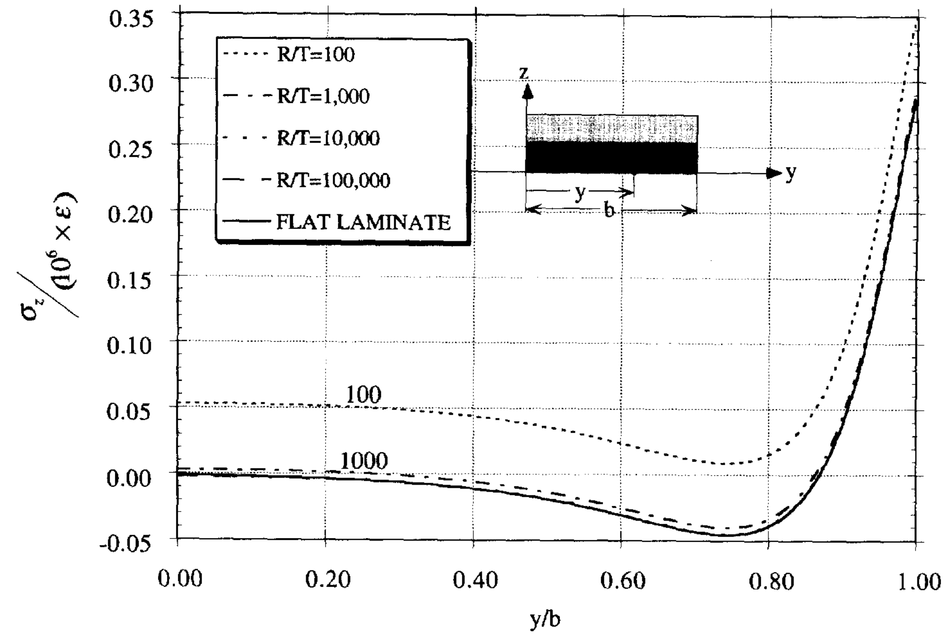

Fig. 4. Transverse normal stress distribution at the 90/90 interface.

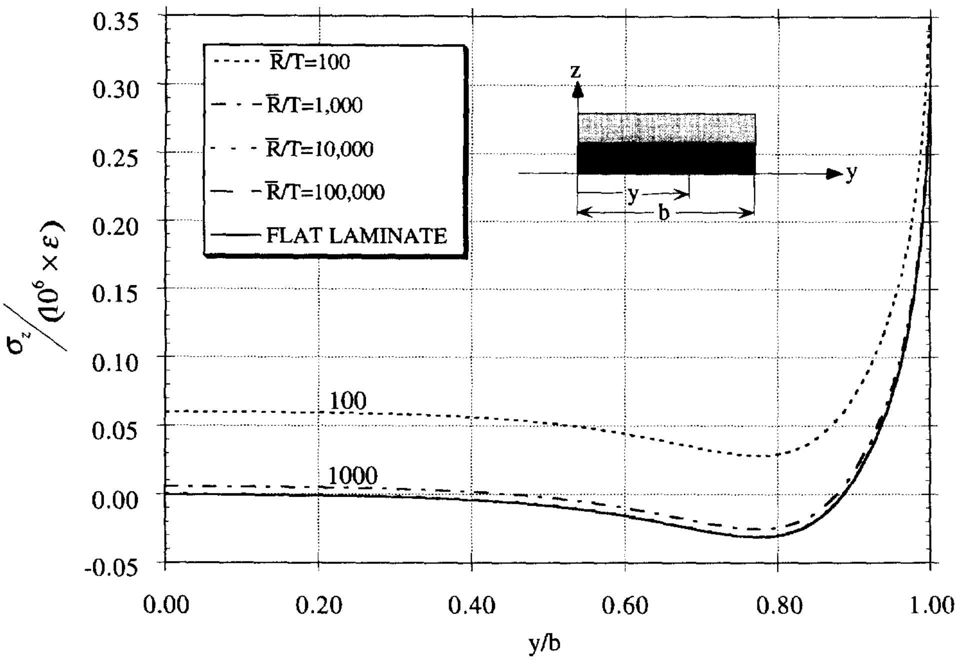

Fig. 5. Transverse normal stress distribution at the 0/90 interface.

0.0042634, respectively. For these two curves, if the ordinate values for all y/b are shifted by an amount equal to these differences, the results for $\bar{R}/T$ of 100 and 1,000 are nearly identical to the flat laminate results. The results of Figs 4–6 clearly indicate that the large radius axisymmetric model provides nearly identical results to the flat laminate model for the predictions of the free edge stresses in flat laminated coupons with transversely isotropic layers.

CRACKED LAMINATE EXAMPLES

Numerical predictions for flat laminates containing delaminations and transverse cracks will now be presented. The damage modeling capability of the large radius formulation was first validated by comparison to a plane strain analytical solution by Konishi

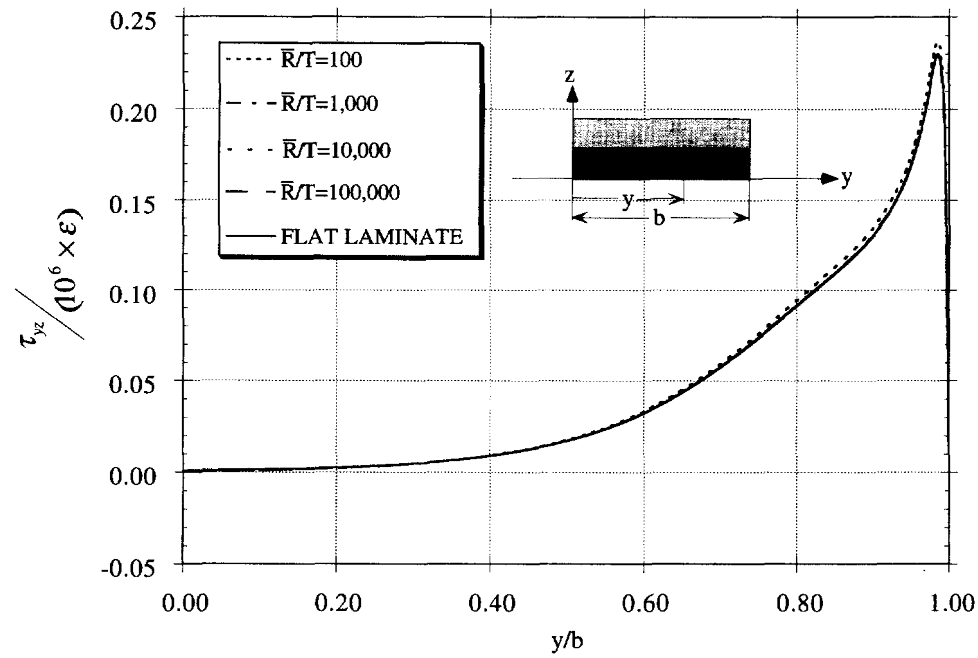

Fig. 6. Transverse shear stress at the 0/90 interface.

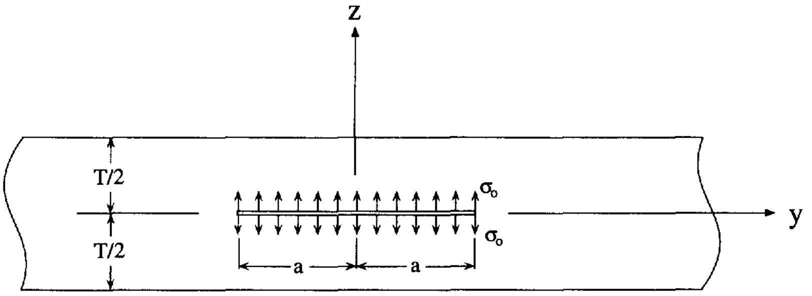

Fig. 7. Pressurized through crack in a flat isotropic body.

and Atsumi (1973). The flat transversely isotropic body of thickness T in the z Cartesian coordinate direction and infinite in the x–y plane contains a pressurized crack of length $2a$ at the mid-surface, as shown in Fig. 7. The body was modeled using quarter symmetry with an $\bar{R}/T$ ratio of 100,000 and a width to thickness ratio of 20. Since plane strain conditions in the hoop direction were required, no artificial external or internal pressure loading was used. The only prescribed non-zero traction was pressure loading normal to the crack face.

Konishi and Atsumi (1973) plotted the normalized mode I stress intensity factor K_I as a function of layer height to crack length for various E_z/E_y moduli ratios and assumed Poisson's ratios $\nu_{yz} = \nu_{zy} = 0.28$. For comparison, the layer thickness and the crack pressure loading were arbitrarily selected as $T/2 = 1.0$ and $\sigma_o = 0.1$.

The stress intensity factor prediction from the large radius model was determined by calculating the energy release rate $\mathcal{G}$. The solution of the boundary value problem has an exponential ξ dependence (Pagano 1991) and $\mathcal{G}$ was calculated directly using differentiation. The relationship given by Sih and Liebowitz (1968) for a homogeneous orthotropic material with a crack parallel to the plane of symmetry (modified for the present notation), provided the stress intensity factor for the calculated energy release rate.

$$\mathcal{G}_I = K_I^2 \left(\frac{b_{11} b_{33}}{2}\right)^{1/2} \left[\left(\frac{b_{33}}{b_{11}}\right)^{1/2} + \frac{2b_{13} + b_{55}}{2b_{11}}\right]^{1/2}. \tag{95}$$

For plane strain we have,

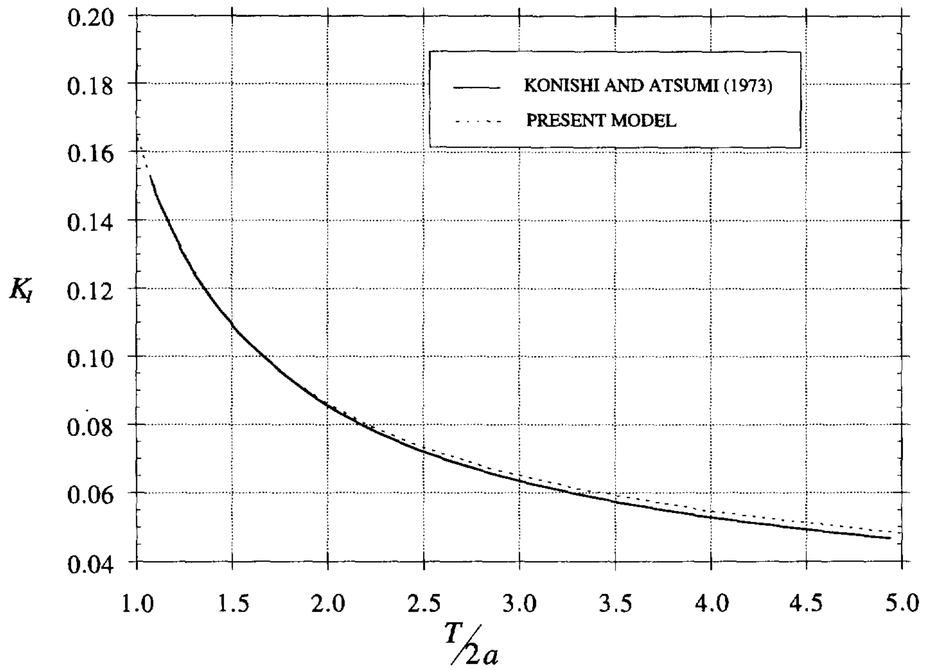

Fig. 8. Plane strain K_I as function of crack width for $E_z/E_y = 0.5$.

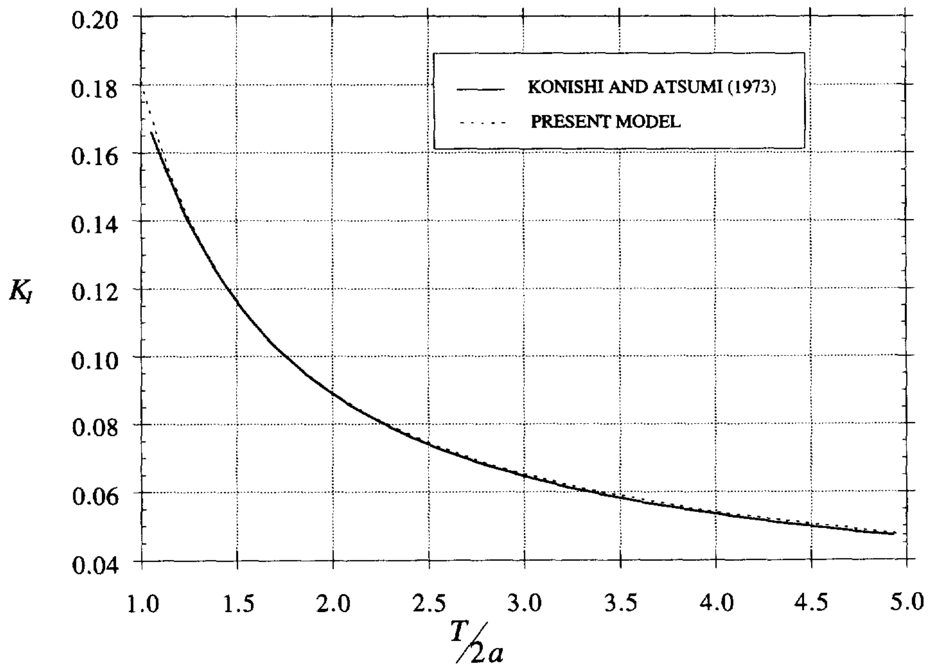

Fig. 9. Plane strain K_I as function of crack width for $E_z/E_y = 1.0$.

$$b_{ij} = a_{ij} - \frac{a_{i2}a_{j2}}{a_{22}}, \quad i,j = 1,2,\ldots,6 \tag{96}$$

where a_{ij} are components of the elastic compliance matrix. Figures 8, 9 and 10 show the stress intensity factor predictions from the analytical solution of Konishi and Atsumi (1973) and the large radius model for E_z/E_y of 0.5, 1.0 and 1.5, respectively.

Using the material properties of the free edge problem above, the stress field ahead of a transverse crack in a $[0/90]_s$ laminate, as shown in Fig. 11, is evaluated. Using an $\bar{R}/T$ ratio of 100,000, the transverse normal and shear stress predictions from the axisymmetric

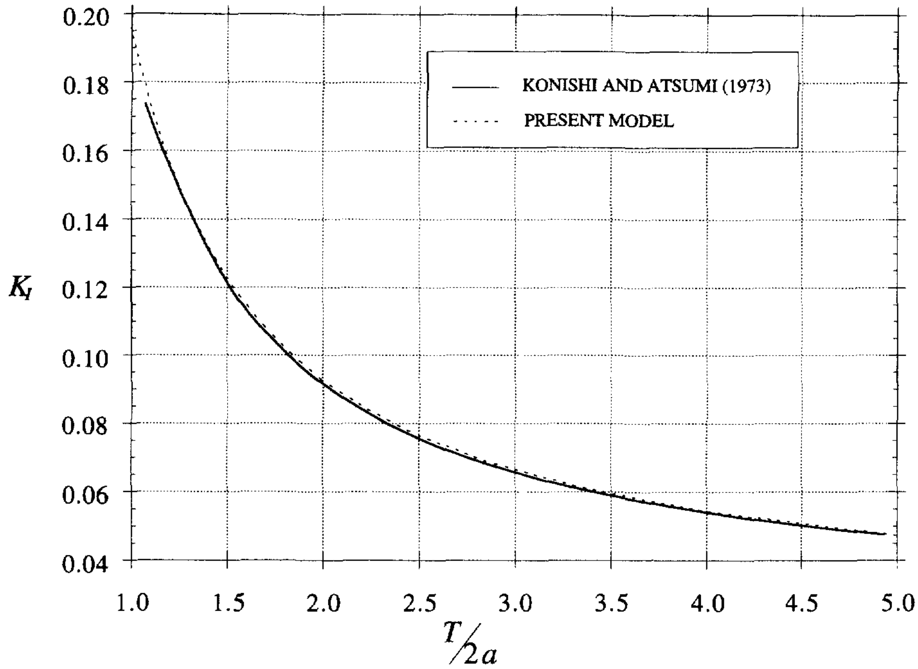

Fig. 10. Plane strain K_I as function of crack width for $E_z/E_y = 1.5$.

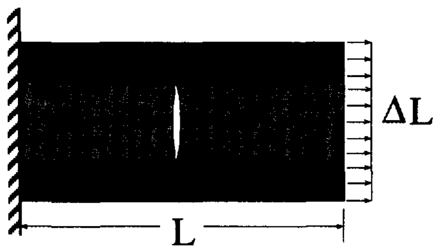

Fig. 11. Transverse crack in cross-ply laminate.

model are compared to those of the flat laminate model ASCA (1992) in Figs 12–14 where it can be seen that the axisymmetric model results are nearly identical to the flat laminate results.

Although delamination is typically preceded by transverse cracking, we will assume here that we have a symmetric cross-ply laminate under uniform axial strain with a through-length midplane delamination, following that of Whitney (1986). Consider a laminate with the following ply properties

$$\frac{E_1}{E_2} = 14.0 \quad \frac{G_{12}}{E_2} = 0.533 \quad \frac{G_{23}}{E_2} = 0.323$$

$$\frac{E_3}{E_2} = 1.0 \quad \nu_{12} = 0.30 \quad \nu_{23} = 0.55.$$

A $[0/90]_s$ laminated coupon containing a free edge delamination and subjected to an axial strain was modeled as a cylinder with $\bar{R}/T = 100{,}000$ subjected to a small positive traction on its exterior. All four lamina of the laminate, shown in Fig. 15 (one quarter of the laminate is shown in the figure), were modeled with the axisymmetric model. The width to thickness ratio $2b/T$ of the laminate is equal to 25. The face of the crack of length $2a$, is traction free. The normalized transverse normal stress distribution ahead of the crack tip for a laminate with $2a/T = 5$ and $N = 6$ is shown in Fig. 16. Considering that the transverse normal stress is singular at the crack tip, the present theory gives strong evidence of the

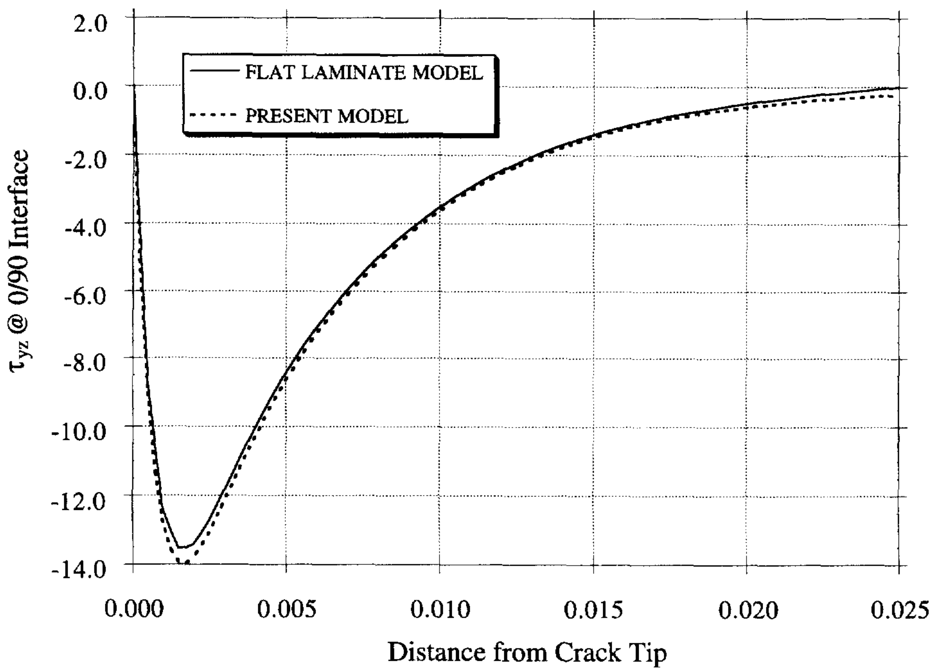

Fig. 12. Transverse shear stress at the 0/90 interface.

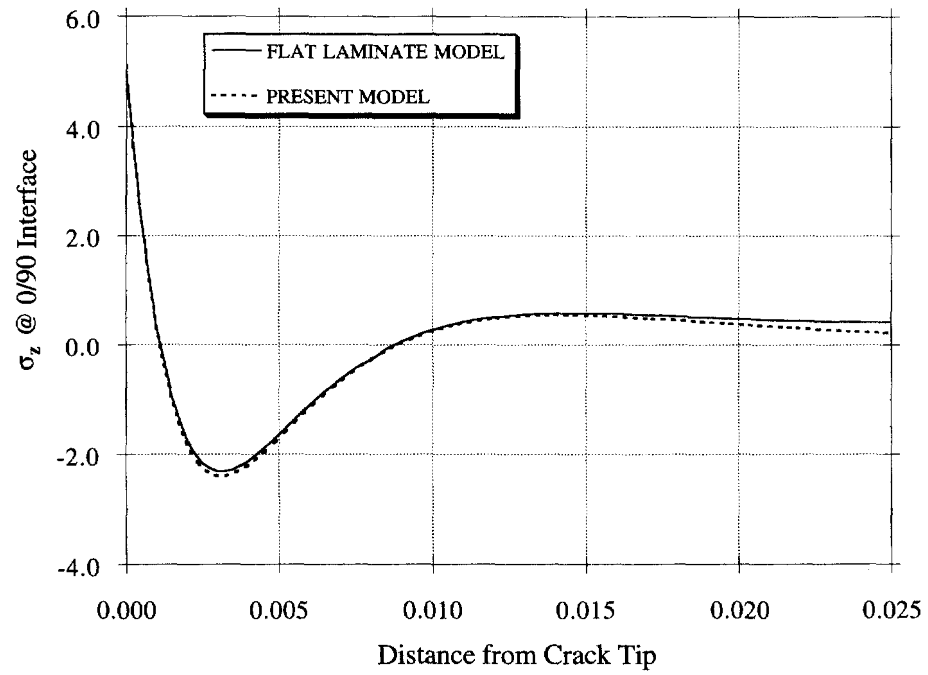

Fig. 13. Transverse normal stress at the 0/90 interface.

singularity due to the extreme stress gradient in the neighborhood of the crack tip and because of the principle of "layer equilibrium" (Pagano 1978a) is equipollent with the known result. The normalized energy release rate as a function of the crack length for $2a/T \leqslant 3$ for the $[0/90]_s$ laminate is shown in Fig. 17. The lower order theories of Whitney (1986), Harikumar and Krishna Murty (1991) and Armanios and Badir (1990), all based on shear deformation theory, all provide equivalent values of $\mathscr{G}$ for crack lengths $2a/T \geqslant 2$ where the energy release rate remains relatively constant. Lamination theory can also accurately predict $\mathscr{G}$ for crack lengths $2a/T \geqslant 2$. However, for crack lengths $2a/T < 2$, these approximate theories are expected to be inaccurate. The total energy release rate for edge

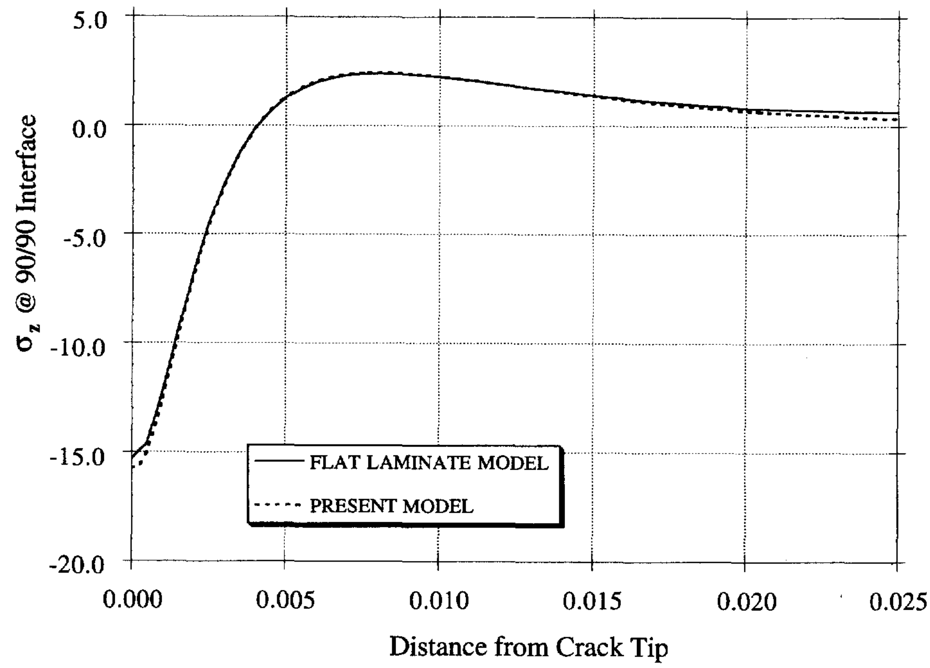

Fig. 14. Transverse normal stress at the 90/90 interface.

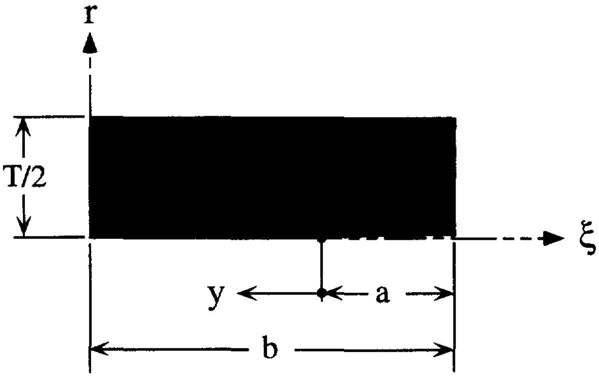

Fig. 15. Free-edge mid-plane delamination.

delamination, as discussed by Sun and Jih (1987) and Raju *et al.* (1988), is well defined. Therefore, oscillatory behavior of the total energy release rate for small crack lengths as shown by Harikumar and Krishna Murty (1991) is not expected. Rather, as shown by Wang (1983), it is expected that the total energy release rate tends to zero monotonically as the crack length tends to zero.

For the present model, the energy release rate prediction for small crack lengths is sensitive to the grading and thickness of the layers adjacent to the crack. It is known that for $2a/T = 0$ the energy release rate is zero. Therefore, it is expected that the energy release rate predictions approach zero with vanishing crack length. Letting t_a be the thickness of the layers directly adjacent to the delamination crack, Table 3 shows the energy release rate predictions for various ratios of $2t_a/T$ for a small crack length $2a/T \approx 10^{-5}$. We see that the energy release rate decreases for decreasing $2t_a/T$. For the present example, with $\bar{R}/T = 100{,}000$ and $2t_a/T = 0.025$, we have a radius to thickness ratio for the layers adjacent to the crack tip of $\bar{R}/t_a = 8.0 \times 10^6$.

CONCLUDING REMARKS

An approximate model to define the two dimensional thermoelastic response of flat finite thickness orthotropic solids, to include discrete damage, has been developed. The

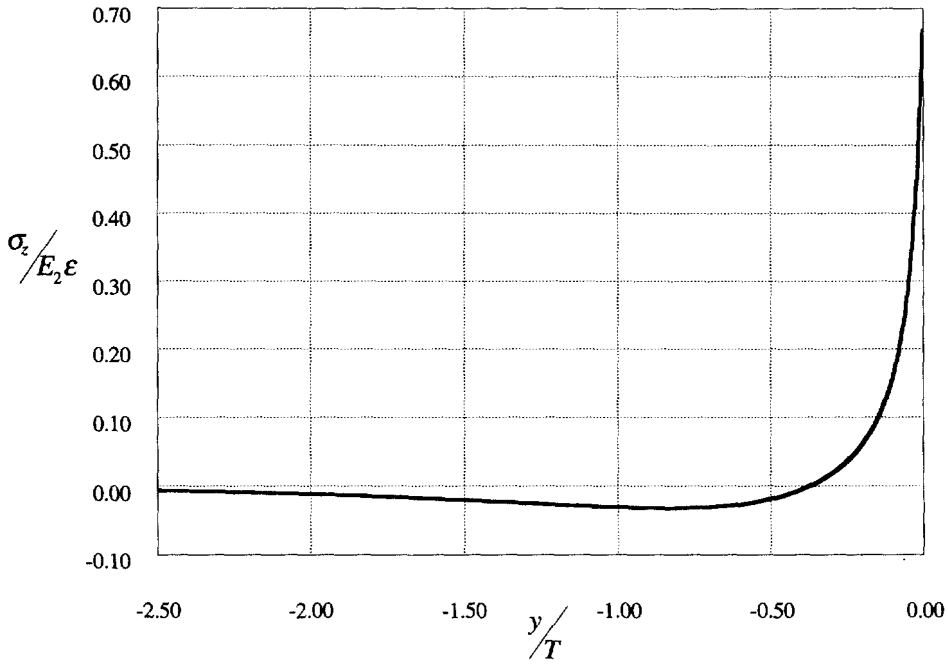

Fig. 16. Transverse normal stress distribution ahead of a crack.

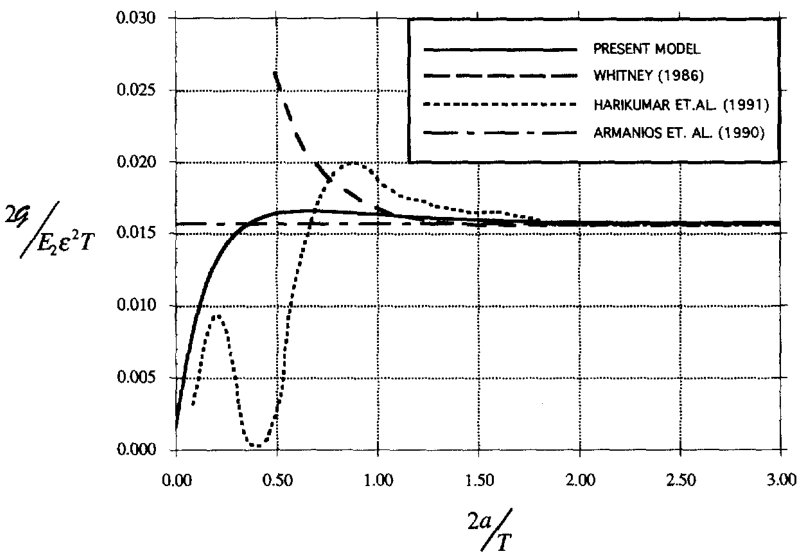

Fig. 17. $\mathscr{G}$ as a function of the delamination width.

Table 3. Normalized $\mathscr{G}$ for various adjacent layer thicknesses

$\frac{2t_a}{T}$	$\frac{2\mathscr{G}}{E_2\varepsilon^2 T}$
0.250	0.002054
$0.1\overline{66}$	0.001579
0.025	0.000289

model has been used to model damage modes in flat laminates. It has been shown that the stress components and the governing equations of the infinite radius model and the flat laminate model are analytically equivalent. However, the solution schemes require the use of the large radius model that has been shown to provide stress field predictions that are nearly identical to those of the flat laminate model in the presence of stress singularities. Inducing a hoop strain in the large radius model, analogous to a prescribed axial strain in the flat laminate model, requires an artificial internal or external pressure that when normalized with respect to the hoop strain is negligible for $\bar{R} \gg T$.

The large radius model is compared to existing flat laminate elasticity solutions for the free-edge stress fields in axially loaded composite coupons. The model is utilized to examine the crack-tip stress field around a transverse crack and a midplane crack for a bi-directional laminate. The distribution of the mode I stress intensity factor versus crack length for transversely isotropic materials compare well with the cited literature and was used to examine the energy release rate distribution for small crack lengths in a cross-ply laminate.

As demonstrated in the transverse crack problem, the model is not limited to primary internal or external pressure loading in the circumferential direction. The model is valid for loading in the axial direction as well as the analysis of pressurized cracks. For problems in which loading in the circumferential direction is not required, constraining radial displacements on planes of constant radius permit for the use of midplane symmetry for laminates with symmetric loading and stacking sequences.

The accuracy of the model can be improved by refining sublayers in the radial direction. The thickness of the layers adjacent to points of singularity have a significant effect on the accuracy of the model. The present model can approximate plane strain conditions in the θ direction for limited cases. Any non-zero radial displacement u indicates a non-zero hoop strain, for $u/\bar{R} \to 0$ however, plane strain conditions can be accurately approximated. Although locally zero hoop strain can be accomplished by constraining the radial displacement on boundaries, currently the large radius model does not allow the hoop strain to be prescribed globally and any radial or axial loading results in non-zero hoop strains.

REFERENCES

Armanios, E. A. and Badir, A. M. (1990) Hygrothermal influence on mode I edge delamination in composites. *Composite structures* **15**(4), 323–342.

ASCA (1992) Automated System for Composite Analysis (ASCA), Adtech Systems Research, Inc., Beavercreek, OH, U.S.A.

Dandan, R. A. (1988) Finite element analysis of laminated composite axisymmetric solids. M.S. thesis, The Ohio State University, U.S.A.

Harikumar, H. K. and Krishna Murty, A. V. (1991) On modelling of laminates containing free-edge delaminations. *Composites Science and Technology* **42,** 393–411.

Konishi, Y. and Atsumi, A. (1973) Crack problem of transversely isotropic strip. *International Journal Engineering Science* **11,** 9–20.

Pagano, N. J. (1971) Stress gradients in laminated composite cylinders. *Journal of Composite Materials* **5,** 260–265.

Pagano, N .J. (1978a) Stress fields in composite laminates. *International Journal of Solids and Structures* **14,** 385–400.

Pagano, N. J. (1978b) Free edge stress fields in composite laminates. *International Journal of Solids and Structures* **14,** 401–406.

Pagano, N. J. (1986) Axisymmetric stress fields in involute bodies of revolution. *Journal of Spacecraft* **23**(2), 165–170.

Pagano, N. J. (1991) Axisymmetric micromechanical stress fields in composites. In *Proceedings* 1991 *IUTAM Symposium on Local Mechanics Concepts for Composite Material Systems*, Springer, Verlag, 1.

Pagano, N. J. and Brown III, H. W. (1993) The full-cell cracking mode in unidirectional brittle matrix composites. *Composites* **24,** 69.

Raju, I. S., Crews, Jr., J. H. and Aminpour, M. A. (1988) Convergence of strain energy release rate components for edge-delaminated composite laminates. *Engineering Fracture Mechanics* **30**(3), 383–396.

Reissner, E. (1950) On a variational theorem in elasticity. *Journal of Mathematics and Physics* **29,** 90–95.

Sandhu, R. S., Sendeckyj, G. P., Schoeppner, G. A. and Pappas, J. E. (1992) Initiation and prevention of edge delamination with and without residual stresses. In *Proceedings of the 74th Meeting of the Structures and Materials Panel AGARD, AGARD-CP*-530, Patras, Greece, 27–28 May 1992, 3-1–3-20.

Sih, G. C. and Liebowitz, H. (1968) Mathematical theories of brittle fracture. In *Fracture, An Advanced Treatise*, Volume II, ed. H. Liebowitz. Academic Press, New York.

Sun, C. T. and Jih, C. J. (1987) On strain energy release rates for interfacial cracks in bi-material media. *Engineering Fracture Mechanics* **28,** 13–20.

Wang, A. S. D. and Crossman, F. W. (1980) Initiation and growth of transverse cracks and edge delamination in composite laminates, I: an energy method. *Journal of Composite Materials* **14**, 21–55.
Wang, S. S. (1983) Fracture mechanics for delamination problems in composite materials. *Journal of Composite Materials* **17**, 210–223.
Whitney, J. M. (1986) Stress analysis of a mode I edge delamination specimen for composite materials. *AIAA Journal* **24**(7), 1164–1168.